EXPERIMENTAL TECHNIQUE FOR DETERMINING SOME DYNAMIC PROPERTIES OF VISCOELASTIC MATERIALS

Amnon Meer

Brown University
Providence, Rhode Island

February 1969

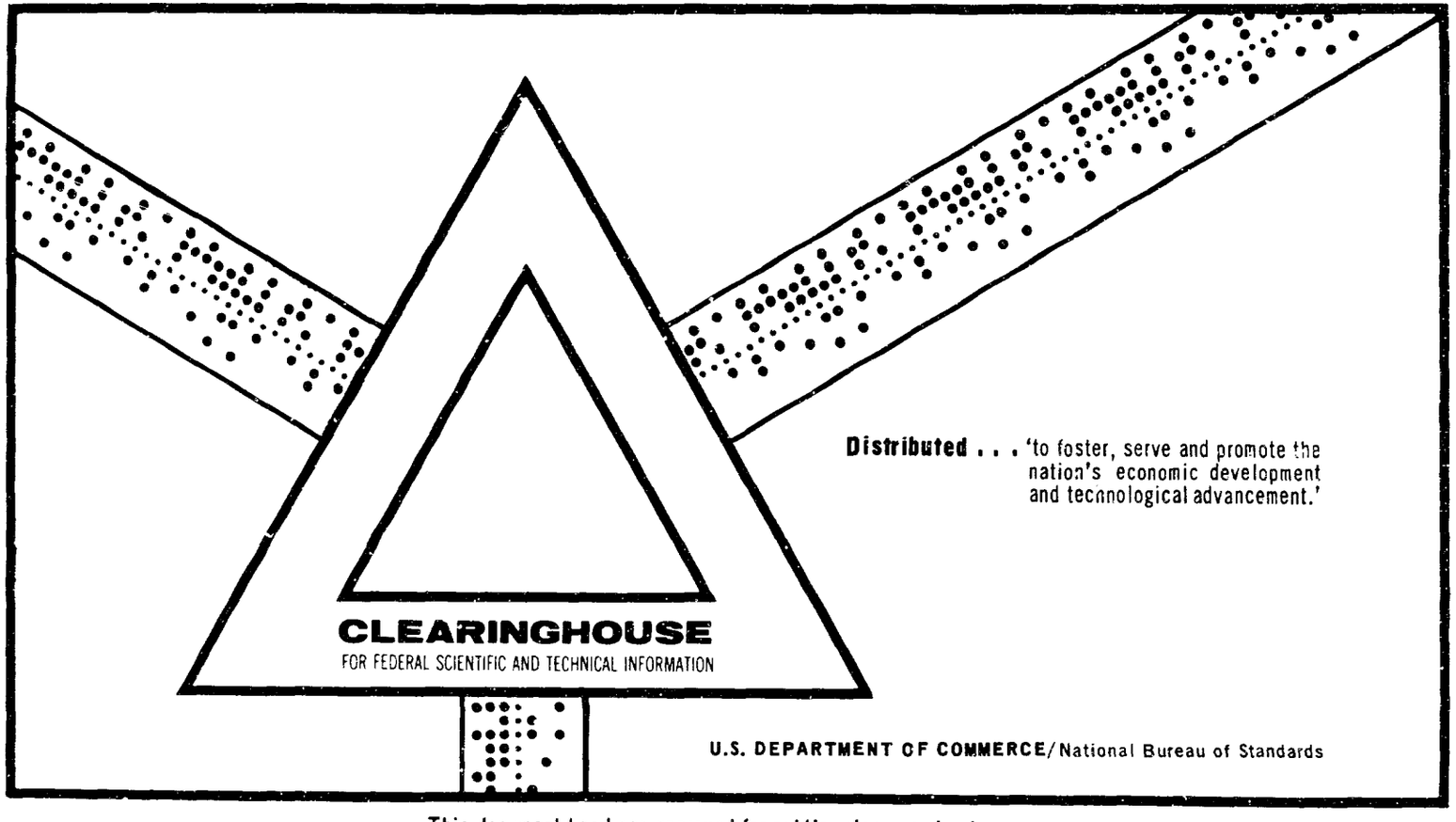

Division

of

Applied Mathematics

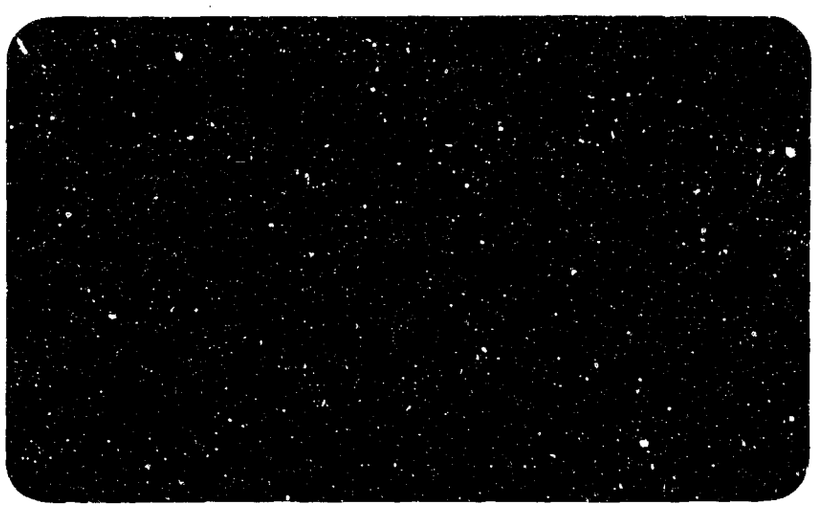

Brown University

Providence

Rhode Island

5606.9-E

Department of the Army

U.S. Army Research Office - Durham

DA-31-124-ARO(D)-358

Technical Report No. 10

Experimental Technique for Determining Some Dynamic Properties of Viscoelastic Materials

by Amnon Meer

DA-358/10

February 1969

Abstract

In this report, an experimental technique is described, by which some basic properties of viscoelastic materials such as phase velocity, loss factor and stress relaxation function could be derived. The technique is based on the propagation and reflection of longitudinal stress pulses in a system of two bars, one of which is elastic with known properties, and the other viscoelastic with properties to be determined. It is shown that the unknown properties of the viscoelastic bar may be determined from the shapes of the incident and reflected stress pulses which travel in the elastic bar. It turns out, however, that the only material property which may be derived with reasonable accuracy is the phase velocity for the basic frequency of the pulses propagating along the bars. All the other material properties proved to be extremely sensitive to small experimental errors and hence no reliable values for them could be derived.

1. Introduction

The subject known as viscoelasticity has developed considerably in recent years. This subject deals with materials whose stress-strain behavior is time dependent for all levels of stress and strain.

The mathematical formulation of the theory of viscoelasticity is well established (see for example references 1-4). The essence of any such formulation is the appropriate mathematical representation of the stress-strain behavior of the viscoelastic material. For most viscoelastic materials undergoing small deformations, the dependence of stress on strain can be well approximated to by a linear relation. In this case there are three basic approaches which are commonly used for describing the stress-strain behavior of a viscoelastic material.

In the first approach, the stress-strain relation is described by a suitable linear differential equation with constant coefficients [2].* In order to describe the behavior of real viscoelastic solids, however, such an equation must involve quite a few terms and this makes any mathematical treatment rather lengthy and in fact impractical. In the second approach, the stress strain relation is described by a suitable hereditary integral [1-4]. Such a representation is based on the Boltzmann superposition principle which holds for linear viscoelastic solids. In this representation, the stress is evaluated from an integral

* Numbers in square brackets refer to the bibliography at the end of the paper.

which includes a certain material property known as the stress relaxation function (or relaxation modulus), and the strain is evaluated from an integral which includes another material property known as the creep function (or creep compliance). The stress-relaxation function describes the stress-time dependence of the material when subjected to a unit step loading of strain. The creep function in contrast describes the strain-time dependence of the material when subjected to a unit step loading of stress. Both properties may be derived for any linear viscoelastic material from fairly simple experiments (see for example, Ferry, pp. 105-150). Such experiments may usually provide reliable data for times which are larger than 1 sec. For times which are much shorter than 1 sec., the stress-strain behavior of the material is best represented by the third approach.

In the third approach, a sinusoidal stress is applied to the material, and the resulting sinusoidal strain is related to the stress through a complex modulus which is dependent on the frequency of the applied oscillations. The absolute value of this complex modulus gives the ratio between the maximum amplitudes of the stress and the strain, whereas the ratio between the imaginary and real parts of this complex modulus, is a measure of the internal friction in the material. There are quite a few experimental methods which have been used in order to determine the complex modulus of viscoelastic materials. Two good summaries of such methods were given by Kolsky [5-6].

In this report, a new technique is described, in which the complex modulus of viscoelastic materials (or alternatively

the phase velocity and loss angle δ which are directly related to it as is shown in appendix I) as well as the stress relaxation function E(t) for short times, may be evaluated. This technique is based on certain phenomena which take place during the arrival of an extensional stress pulse at the interface between two long bars made of different materials. It is known (see for example Kolsky and Lee [7]) that an extensional stress pulse impinging on the boundary between two elastic rods, will split into two extensional pulses, namely a reflected and a transmitted pulse. The amplitudes of the reflected and transmitted pulses are related to that of the incident pulse by a certain characteristic impedance ratio which is evaluated in the context of this report (see also Kolsky and Lee [7]). However the shapes of all three pulses will remain similar.

This situation no longer exists when one or both of the bars are viscoelastic. In this case, as was shown by Kolsky and Lee [7], not only the amplitudes but also the shapes of the reflected and transmitted pulses will in general differ from that of the incident pulse. The changes in pulse shapes are strictly dependent on the particular properties of the materials involved. Hence by analysing these changes by a suitable mathematical procedure, the desired viscoelastic properties may be derived. The phenomenon of reflection and transmission just described and its implied consequences, form the basis of the experimental technique described in this report.

2. General Description of Technique

In the experimental technique described in this report, two bars, one of which was elastic with known properties and the other viscoelastic with properties to be determined, were placed end to end. This was done either by applying a thin layer of grease between the two bars and pressing them together or by gluing one bar on top of the other.

The two bars were held in a vertical position, with the elastic bar on top of the viscoelastic bar. A small steel ball was dropped onto the top surface of the upper bar. The impact produced a mechanical pulse which was propagated along this bar towards the lower bar. At the interface between the two bars, reflected and transmitted pulses were generated. Recording of all three pulses (the incident pulse, the reflected pulse and the transmitted pulse) was carried out by means of electrical resistance strain gages which were bonded to the surface of the bars at different locations. The strain gage outputs were fed on to a cathode-ray oscillograph where they were amplified and the traces recorded photographically. The photographic images thus obtained were first magnified by the use of a slide projector and the enlarged pictures were traced with a pencil.

The incident and reflected pulse shapes were later analysed mathematically with the aid of a Fourier analysis or alternatively by a Laplace transform method. (It is shown in this report that a mathematical analysis of the transmitted pulse is not required.) From such an analysis, as is shown in this report, the unknown

material properties of the viscoelastic bar, such as C (the phase velocity), tan δ (the loss factor) and E(t) (the stress relaxation function) could theoretically be derived.

3. Theoretical Background and Analysis

3.1. Elastic Bars

In trying to find material properties of an unknown material by means of the experimental technique previously described, let us start our investigation with the relatively simple case of two elastic bars attached together.

Consider an extensional wave of arbitrary shape traveling from one elastic bar to another. Upon reaching the boundary between the two bars, this wave will, in general generate a reflected pulse and a transmitted pulse. Let the displacements associated with the incident, the reflected and the transmitted pulses be denoted by u_1, u_2 and u_3 respectively.

Assuming the incident pulse to travel in the direction of increasing x where x is the longitudinal coordinate measured along the axis of the bar, we may then write:

$$\begin{aligned} u_1 &= f(t - \frac{x}{C_1}) \\ u_2 &= F(t + \frac{x}{C_1}) \\ u_3 &= G(t - \frac{x}{C_2}) \end{aligned} \tag{1}$$

where C_1 and C_2 are the wave velocities in the first and second bar respectively. The relations between the functions f, F, and G may be inferred from the conditions of the continuity of displacements and stresses across the boundary which will be hitherto designated as x=0 for the sake of convenience. We thus have:

$$\begin{aligned} u_1 + u_2 &= u_3 \\ \sigma_1 + \sigma_2 &= \sigma_3 \end{aligned} \qquad \text{at } x=0$$

(Here σ denotes stress).

Applying Hooke's law to the second condition, and using expression (1) for the displacements one gets at x=0

$$\begin{aligned} f(t) + F(t) &= G(t) \\ E_1[-\tfrac{1}{C_1}f'(t) + \tfrac{1}{C_1}F'(t)] &= -E_2\,\tfrac{1}{C_2}G'(t) \end{aligned} \qquad (2)$$

where the dash denotes differentiation with respect to the argument. Here E_1 and E_2 are Young's moduli in the first and second rod respectively, in which case we have $C_1^2 = \frac{E_1}{\rho_1}$ and $C_2^2 = \frac{E_2}{\rho_2}$, ρ_1 and ρ_2 being the corresponding densities.

Differentiating the first equation in (2) w.r.t. time and solving for the two unknowns F'(t) and G'(t), one gets:

$$F'(t) = \frac{\rho_1 C_1 - \rho_2 C_2}{\rho_1 C_1 + \rho_2 C_2} f'(t)$$

$$G'(t) = \frac{2\rho_1 C_1}{\rho_1 C_1 + \rho_2 C_2} f'(t)$$

Integrating the last equations w.r.t. time, and assuming zero initial conditions, one gets:

$$\begin{aligned} F(t) &= \frac{\rho_1 C_1 - \rho_2 C_2}{\rho_1 C_1 + \rho_2 C_2} f(t) \\ G(t) &= \frac{2\rho_1 C_1}{\rho_1 C_1 + \rho_2 C_2} f(t) \end{aligned} \qquad (3)$$

Equations (3) give us the existing relations between the three functions f, F, and G which describe the displacements of the pulses. Observing that at the boundary x=0, $u_1 = f(t)$, $u_2 = F(t)$ and $u_3 = G(t)$, we may deduce the following relations between the displacement amplitudes:

$$\frac{u_2}{u_1} = \frac{\rho_1 C_1 - \rho_2 C_2}{\rho_1 C_1 + \rho_2 C_2}$$
$$\frac{u_3}{u_1} = \frac{2\rho_1 C_1}{\rho_1 C_1 + \rho_2 C_2} \qquad (4)$$

at x=0 and for any time t within the time interval at which reflection and transmission take place at the boundary. In the experimental procedure, however, the quantities which were being measured were strains rather than displacements.

In order to find the appropriate relations between the strain amplitudes, let us first derive the corresponding strains from expressions (1) and (3). We then will have at x=0:

$$\varepsilon_1 = \frac{\partial u_1}{\partial x}\Big|_{x=o} = -\frac{1}{C_1} f'(t)$$

$$\varepsilon_2 = \frac{\partial u_2}{\partial x}\Big|_{x=o} = \frac{1}{C_1} F'(t) = \frac{1}{C_1} \frac{\rho_1 C_1 - \rho_2 C_2}{\rho_1 C_1 + \rho_2 C_2} f'(t)$$

$$\varepsilon_3 = \frac{\partial u_3}{\partial x}\Big|_{x=o} = -\frac{1}{C_2} G'(t) = -\frac{1}{C_2} \frac{2\rho_1 C_1}{\rho_1 C_1 + \rho_2 C_2} f'(t)$$

Thus the existing relations between the strain amplitudes, at x=0 and for all times within the time interval at which reflection and transmission take place, will be as follows:

$$\frac{\varepsilon_2}{\varepsilon_1} = -\frac{\rho_1 C_1 - \rho_2 C_2}{\rho_1 C_1 + \rho_2 C_2} = \frac{\rho_2 C_2 - \rho_1 C_1}{\rho_2 C_2 + \rho_1 C_1}$$

$$\frac{\varepsilon_3}{\varepsilon_1} = \left(\frac{C_1}{C_2}\right) \frac{2\rho_1 C_1}{\rho_1 C_1 + \rho_2 C_2} \qquad (5)$$

Expressions (4) and (5) show us that the various relations between the pulses are determined by the corresponding characteristic impedances ρC but the velocity ratio $\frac{C_1}{C_2}$ also appears in the relations for strains.

3.2. Viscoelastic Bars

Having discussed the case of two elastic bars, we may now proceed to the more complicated case of two viscoelastic bars attached together.

As a starting point for the analysis we will first consider the case of an extensional harmonic wave of some known frequency traveling from one viscoelastic bar to another. As in the case of the two elastic bars, this situation will again result in the generation of two pulses at the boundary, namely a reflected pulse and a transmitted pulse. Denoting the displacements associated with the incident, the reflected and the transmitted pulses by u_i, u_r and u_t respectively, we may then write (see appendix I):

$$u_i = A \exp[-\alpha_1 x + ip(t - \frac{x}{C_1})]$$

$$u_r = B \exp[+\alpha_1 x + ip(t + \frac{x}{C_1})] \qquad (6)$$

$$u_t = T \exp[-\alpha_2 x + ip(t - \frac{x}{C_2})]$$

Here α_1 and α_2 are the attenuation coefficients in the first and second bar respectively and C_1 and C_2 are the corresponding phase velocities at the given frequency p.

A, B and T are in general complex so that

$$A = A_1+iA_2, \quad B = B_1+iB_2 \text{ , and } \quad T = T_1+iT_2$$

where $A_1, A_2, B_1, B_2, T_1, T_2$ are the amplitudes of the displacements at the interface x=0.

From the simple one dimensional theory of wave propagation in viscoelastic materials (see appendix I), we have the following expressions for the attentuation α and the phase velocity C in a viscoelastic material:

$$\alpha = \frac{p}{C} \tan \frac{\delta}{2}$$

$$C = \sqrt{\frac{E^*}{\rho}} \sec \frac{\delta}{2}$$

Here ρ is the density and:

$$\tan \delta = \frac{E_2}{E_1} \qquad E^* = \sqrt{E_1^2+E_2^2}$$

where E_1+iE_2 is the complex Young's modulus of the material (see for example Ferry [3]). For most viscoelastic materials, commonly used we have

$$\tan^2 \delta << 1$$

In this case we may write the following approximations:

$$C \simeq \sqrt{\frac{E^*}{\rho}} \simeq \sqrt{\frac{E_1}{\rho}}$$

$$\alpha \simeq \frac{p \tan \delta}{2C} \qquad (7)$$

The existing relations between the displacement amplitudes $A_1,\ldots,T_2$ may again be found by applying the conditions of the continuity of displacements and stresses across the boundary. This indeed was done by Kolsky and Lee [7] who found the following relations (see Kolsky and Lee, p. 25):

$$
\begin{aligned}
B_1 &= \frac{1-s}{1+s} A_1 + \frac{2s(\delta_2-\delta_1)}{(1+s)^2} A_2 \\
B_2 &= \frac{2s(\delta_1-\delta_2)}{(1+s)^2} A_1 + \frac{1-s}{1+s} A_2 \\
T_1 &= \frac{2}{1+s} + \frac{2s(\delta_2-\delta_1)}{(1+s)^2} A_2 \\
T_2 &= \frac{2s(\delta_1-\delta_2)}{(1+s)^2} A_1 + \frac{2}{1+s} A_2
\end{aligned}
\tag{8}
$$

Here:

$$
\begin{aligned}
s &= \frac{\rho_2 C_2}{\rho_1 C_1} \\
\delta_1 &= \frac{1}{2} \tan \delta \\
\delta_2 &= \frac{1}{2} \tan \delta'
\end{aligned}
$$

where δ and δ' are the phase angles between a harmonic stress and the corresponding harmonic strain, in the first and second bar respectively.

For our purposes, however, we are more interested in expressing the material properties of the second bar in terms of the displacement amplitudes, since the latter (as will be shown later in the analysis) are directly related to the strains which in turn will be measured by experiment.

In order to find an expression for the material properties of the second bar, one might use expressions (8) and through some algebraic manipulations arrive at some complicated formulas relating δ_2 and s to the known quantities $A_1, A_2, B_1, B_2, \delta_1$. Another way of finding out the desired relations between material properties and displacement amplitudes will be to start again with the same analysis presented by Kolsky and Lee [7], and then arrive directly at the desired relations through some intermediate step in the analysis. The second approach will be presented here as it results in somewhat simpler relations between the material properties of the second bar and the displacement amplitudes.

We may now start our analysis by writing down the boundary conditions for the displacements and stresses across the boundary x=0:

$$\begin{aligned} u_i + u_r &= u_t \\ \sigma_i + \sigma_r &= \sigma_t \end{aligned} \qquad \text{at } x=0 \qquad (9)$$

The stresses σ_i, σ_r, and σ_t may be derived from expression (6) using the following relations:

$$\begin{aligned} \sigma_i &= (E_1+iE_2)\frac{\partial u_i}{\partial x} \\ \sigma_r &= (E_1+iE_2)\frac{\partial u_r}{\partial x} \\ \sigma_t &= (E_1'+iE_2')\frac{\partial u_t}{\partial x} \end{aligned} \qquad (10)$$

Here E_1+iE_2 is the complex Young's modulus in the first rod and $E_1'+iE_2'$ is the corresponding modulus in the second rod. Substitution of the displacements and stresses from expressions (6) and

(10) in the boundary conditions (9) yields the following relations:

$$\text{(a)} \quad A_1 + B_1 = T_1$$

$$\text{(b)} \quad A_2 + B_2 = T_2 \qquad (11)$$

$$\text{(c)} \quad (E_1+iE_2)[(-\alpha_1 - \frac{ip}{C_1})(A_1+iA_2)+(\alpha_1+\frac{ip}{C_1})(B_1+iB_2)]$$
$$= (E_1'+iE_2')(-\alpha_2 - \frac{ip}{C_2})(T_1+iT_2)$$

Now:

$$E_2 = E_1 \tan \delta$$
$$E_2' = E_1' \tan \delta'$$

$$\alpha_1 = \frac{p \tan \delta}{2C_1}$$

$$\alpha_2 = \frac{p \tan \delta'}{2C_2}$$

Also:

$$\delta_1 = \frac{1}{2} \tan \delta$$

$$\delta_2 = \frac{1}{2} \tan \delta'$$

$$S = \frac{E_1'C_1}{C_1C_2} = \frac{\rho_2 C_2}{\rho_1 C_1}$$

If we now make these substitutions in equation (11c), equate real and imaginary parts and neglect terms involving $\tan^2\delta$ w.r.t. unity, we obtain the following two relations:

$$(A_1-B_1)\delta_1 + (A_2-B_2) = S(T_1\delta_2+T_2)$$
$$(A_1-B_1) - (A_2-B_2)\delta_1 = S(T_1-T_2\delta_2) \tag{12}$$

Substitution of the amplitudes T_1 and T_2 from expressions (11a) and (11b) in the two equations (12) yields:

$$(A_1-B_1)\delta_1 + (A_2-B_2) = S(A_1+B_1)\delta_2 + S(A_2+B_2)$$
$$(A_1-B_1) - (A_2-B_2)\delta_1 = S(A_1+B_1) - S(A_2+B_2)\delta_2 \tag{13}$$

The last two equations can be solved algebraically for the two unknowns δ_2 and S. When this is done, and upon replacing δ_1 and δ_2 by $\frac{1}{2}\tan\delta$ and $\frac{1}{2}\tan\delta'$ one gets:

$$\tan\delta' = \frac{(A_1^2+A_2^2-B_1^2-B_2^2)\tan\delta + 4(A_2B_1-A_1B_2)}{(A_1^2+A_2^2-B_1^2-B_2^2) + (A_1B_2-A_2B_1)\tan\delta}$$
$$S = \frac{\rho_2 C_2}{\rho_1 C_1} = \frac{(A_1^2+A_2^2-B_1^2-B_2^2) + (A_1B_2-A_2B_1)\tan\delta}{(A_1+B_1)^2 + (A_2+B_2)^2} \tag{14}$$

Expressions (14) give us the desired relations between the material properties of the second bar, namely $\tan\delta'$ and C_2 and the displacement amplitudes of the incident and reflected pulses.

It is worth noting that the displacement amplitudes of the transmitted pulse do not enter into these relations. Hence in carrying out experiments which are directed towards the evaluation of material properties of the second bar, no measurements have to be taken on that bar. The only measurements required are those obtained from the first bar. This last fact is of extreme

importance when one is trying to determine mechanical properties of materials of very large damping where direct propagation measurements are impractical, or materials like rubber or clay to which regular measurement techniques (such as strain gages) are very difficult to apply.

Having now found the desired relations between the material properties of the second bar, and the displacement amplitudes and material properties in the first bar for a sinusoidal wave at an angular frequency p, we may now try to evaluate those relations for the case of a general pulse of arbitrary shape and duration. In order to do this we must first give the displacement pulse a suitable representation. This might be done by writing the appropriate pulse in terms of a Fourier integral. Thus we may write the incident pulse, the reflected pulse and the transmitted pulse as:

$$
\begin{aligned}
u_i &= \mathrm{Re} \int_0^\infty (A_1' + iA_2') e^{-\alpha_1 x + ip\left(t - \frac{x}{C_1}\right)} dp \\
u_r &= \mathrm{Re} \int_0^\infty (B_1' + iB_2') e^{+\alpha_1 x + ip\left(t + \frac{x}{C_1}\right)} dp \\
u_t &= \mathrm{Re} \int_0^\infty (T_1' + iT_2') e^{-\alpha_2 x + ip\left(t - \frac{x}{C_2}\right)} dp
\end{aligned}
\qquad (15)
$$

The displacements described by expressions (15) are no more than the generalization of the displacements given in expressions (6) for the case of an infinite range of continuous frequency spectrum. For the purpose of numerical computations, however, it is necessary to represent the pulses in the form of Fourier

sums rather than Fourier integrals. Thus we can write the three pulses as:

$$
\begin{aligned}
u_i &= \mathrm{Re} \sum_{k=o}^{\infty} (A_1+iA_2)e^{-\alpha_1 x+ikp_o(t-\frac{x}{C_1})} \\
u_r &= \mathrm{Re} \sum_{k=o}^{\infty} (B_1+iB_2)e^{+\alpha_1 x+ikp_o(t+\frac{x}{C_1})} \\
u_t &= \mathrm{Re} \sum_{k=o}^{\infty} (T_1+iT_2)e^{-\alpha_2 x+ikp_o(t-\frac{x}{C_2})}
\end{aligned}
\qquad (16)
$$

In the last representation we have chosen some basic frequency p_o and then described all the pulses as periodic functions with period $T_o = \frac{2\pi}{p_o}$, and Fourier coefficients $A_1,\ldots,T_2$. We must therefore observe that the pulse representation given by (16) is not the same as that given by (15). The latter mathematically describes a pulse whereas the first one describes a periodic function with period T_o.

However, within the time interval from zero to T_o, both representations are equivalent, namely they describe exactly one unique pulse. Hence, in using expression (16) for further analysis, we must restrict ourselves to times which are not less than zero and not greater than T_o.

The basic period T_o should be chosen so as to be long enough to contain the whole of the pulse, but also small enough to insure fast convergence of the Fourier sum to its final value.

If we now examine the displacements described by expressions (16), we see that they are no more than linear sums of expressions similar to those given in (6). Since we are dealing with linear viscoelasticity, relations (8) and (14) must hold for each set of displacement amplitudes (or Fourier coefficients) $A_1,\ldots,T_2$ corresponding to a certain discrete frequency kp_o. Thus in order to find the material properties of the second bar in the case of two general incident and reflected pulses, we must first find the Fourier coefficients of these two pulses by a Fourier analysis technique, and then use relations (14) for each set of Fourier coefficient corresponding to a certain discrete frequency kp_o. In this manner we may get the material properties of the second bar, namely $\tan \delta'$ and C_2 as a function of frequency for frequency values which are integer multiples of the basic frequency p_o. From the analysis we had so far we could find the existing relations between the material properties of the second bar and the displacement amplitudes in the first bar. However, in the experimental technique described in this report, the quantities being measured were strains rather than displacements. Hence it would seem appropriate to carry on the analysis one step further and evaluate the relations between the material properties of the second bar and the strains in the first bar.

In order to do this we must first derive appropriate expressions for the strain pulses traveling in the first bar. This might be done by referring to the incident and reflected

displacement pulses described in expressions (16) and differentiating them w.r.t. x.

Denoting by ε_i and ε_r the resulting incident and reflected strain pulses, we may then write at x=0:

$$\varepsilon_i|_{x=o} = \mathrm{Re} \sum_{k=o}^{\infty} (-\alpha_1 - \frac{ikp_o}{C_1})(A_1+iA_2)e^{ikp_o t} =$$

$$= \sum_{k=o}^{\infty} [(-\alpha_1 A_1 + \frac{kp_o}{C_1} A_2)\cos kp_o t + (\alpha_1 A_2 + \frac{kp_o}{C_1} A_1)\sin kp_o t] \tag{17}$$

$$\varepsilon_r|_{x=o} = \mathrm{Re} \sum_{k=o}^{\infty} (+\alpha_1 + \frac{ikp_o}{C_1})(B_1+iB_2)e^{ikp_o t} =$$

$$= \sum_{k=o}^{\infty} [(\alpha_1 B_1 - \frac{kp_o}{C_1} B_2)\cos kp_o t + (-\alpha_1 B_2 - \frac{kp_o}{C_1} B_1)\sin kp_o t]$$

Expressions (17) might be recognized as Fourier series expansions of the incident and reflected strain pulses at x=0.

Thus if we call the Fourier cosine coefficients and the Fourier-sine coefficients of the incident strain pulse, a_{kc} and a_{ks} respectively, and those of the reflected strain pulse b_{kc} and b_{ks} respectively, we must then have:

$$\begin{aligned} -\alpha_1 A_1 + \frac{kp_o}{C_1} A_2 &= a_{kc} \\ \alpha_1 A_2 + \frac{kp_o}{C_1} A_1 &= a_{ks} \\ \alpha_1 B_1 - \frac{kp_o}{C_1} B_2 &= b_{kc} \\ -\alpha_1 B_2 - \frac{kp_o}{C_1} B_1 &= b_{ks} \end{aligned} \tag{18}$$

Solving the first pair of equations for the displacement amplitudes A_1, A_2, and the second pair of equations for the displacement amplitudes B_1, B_2, and also using the relation $\alpha_1 = \frac{(kp_o)\tan\delta}{2C_1}$ one gets:

$$A_1 = \left(\frac{C_1}{kp_o}\right) \frac{-\frac{\tan\delta}{2} a_{kc} + a_{ks}}{1 + \left(\frac{\tan\delta}{2}\right)^2}$$

$$A_2 = \left(\frac{C_1}{kp_o}\right) \frac{a_{kc} + \frac{\tan\delta}{2} a_{ks}}{1 + \left(\frac{\tan\delta}{2}\right)^2} \qquad (19)$$

$$B_1 = \left(\frac{C_1}{kp_o}\right) \frac{\frac{\tan\delta}{2} b_{kc} - b_{ks}}{1 + \left(\frac{\tan\delta}{2}\right)^2}$$

$$B_2 = -\left(\frac{C_1}{kp_o}\right) \frac{b_{kc} + \frac{\tan\delta}{2} b_{ks}}{1 + \left(\frac{\tan\delta}{2}\right)^2}$$

Inserting the last expressions for the displacement amplitudes in relations (14) and doing some algebraic manipulations, we finally get:

$$\tan\delta' = \frac{(a_{kc}^2 + a_{ks}^2 - b_{kc}^2 - b_{ks}^2)\tan\delta - 4(a_{kc}b_{ks} - a_{ks}b_{kc})}{(a_{kc}^2 + a_{ks}^2 - b_{kc}^2 - b_{ks}^2) + (a_{kc}b_{ks} - a_{ks}b_{kc})\tan\delta}$$

$$S = \frac{\rho_2 C_2}{\rho_1 C_1} = \frac{(a_{kc}^2 + a_{ks}^2 - b_{kc}^2 - b_{ks}^2) + (a_{kc}b_{ks} - a_{ks}b_{kc})\tan\delta}{(a_{kc} - b_{kc})^2 + (a_{ks} - b_{ks})^2} \qquad (20)$$

Expressions (20) give us the desired relations between the material properties of the second bar and the strain amplitudes

(or Fourier coefficients) in the first bar for all frequencies $kp_o (k=1,2,\ldots)$.

3.3. Elastic to Viscoelastic Bar

In the theoretical analysis presented so far we have evaluated some basic relations which exist between strain amplitudes and material properties in one bar, and material properties of a second bar which is attached to the first one. When both bars are elastic, these relations are given by the first expression in (5). When both bars are viscoelastic, these relations are given by expressions (20). When the first bar (namely the one in which the incident and reflected strain pulses are traveling) is elastic, and the second bar is viscoelastic, these relations can be obtained from expression (20) by putting $\tan \delta = 0$. In this case we get:

$$\tan \theta' = \frac{-4(a_{kc}b_{ks}-a_{ks}b_{kc})}{a_{kc}^2+a_{ks}^2-b_{kc}^2-b_{ks}^2}$$

$$S = \frac{\rho_2 C_2}{\rho_1 C_1} = \frac{a_{kc}^2+a_{ks}^2-b_{kc}^2-b_{ks}^2}{(a_{kc}-b_{kc})^2 + (a_{ks}-b_{ks})^2} \qquad (21)$$

where again a_{kc} and a_{ks} are the Fourier cosine coefficients and Fourier sine coefficients of the incident strain pulse, and b_{kc} and b_{ks} are the corresponding coefficients of the reflected strain pulse. When the first bar is elastic and the second bar is viscoelastic, we can also derive an additional expression which will relate the material properties and strain pulses in

the first bar to another material property of the second bar, namely the stress relaxation function E(t). (For the definition of E(t) see for example Flügge, p. 23.) In order to do this we must solve an initial-boundary-value problem of pulse propagation in a system of two bars attached together, one of which is elastic and the other viscoelastic.

Consider an extensional pulse traveling along an elastic bar and reaching the boundary between this bar and a viscoelastic bar attached to it. As was already mentioned earlier, this pulse after being reflected at the interface will generate two additional pulses, namely a reflected pulse and a transmitted pulse. Let us again denote the displacements associated with the incident, the reflected and the transmitted pulses by u_i, u_r, and u_t respectively. The equations of motion for all three pulses may then be written as:

$$\frac{\partial^2 u_i}{\partial t^2} = \frac{1}{\rho_1} \frac{\partial \sigma_i}{\partial x}$$

$$\frac{\partial^2 u_r}{\partial t^2} = \frac{1}{\rho_1} \frac{\partial \sigma_r}{\partial x} \qquad (22)$$

$$\frac{\partial^2 u_t}{\partial t^2} = \frac{1}{\rho_2} \frac{\partial \sigma_t}{\partial x}$$

where as before, σ denotes stress, ρ denotes density, x denotes distance along the bar axis, and t denotes time.

For the sake of convenience we shall consider the initial time t=0 to be the time at which the head of the incident pulse has just reached the interface, and the two other pulses have just started being formed.

The positive x axis will be chosen to point in the direction of the viscoelastic bar, and the origin x=0 will again be assumed to be in the interface between the two bars. In order to solve the equations of motion (22) we must first write down the constitutive relations for each one of the three pulses. For the incident and reflected pulses, since they are propagating in an elastic medium, these relations are simply Hooke's law, namely:

$$\sigma_i = E_1 \frac{\partial u_i}{\partial x}$$
$$\sigma_r = E_1 \frac{\partial u_r}{\partial x} \qquad (23)$$

Here E_1 is Young's modulus in the elastic bar. For the transmitted pulse, since it is propagating in a viscoelastic medium, the constitutive relation may be formulated in terms of a hereditary integral (see for example Flügge, p. 24), namely:

$$\sigma_t(t) = \int_{-\infty}^{t} E_2(t-\tau) \frac{\partial \varepsilon_t}{\partial \tau} d\tau = \int_{-\infty}^{t} E_2(t-\tau) \frac{\partial^2 u_t}{\partial x \partial \tau} d\tau \qquad (24)$$

Here ε_t is the transmitted strain and $E_2(t-\tau)$ is the stress relaxation function in the viscoelastic bar at the time $t-\tau$. If all the pulses with which we are dealing are assumed to be smooth functions of time, then $\frac{\partial \varepsilon_t}{\partial \tau}$ is zero for all times between $-\infty$ and 0^+ and hence relation (24) may be written as:

$$\sigma_t(t) = \int_{0^+}^{t} E_2(t-\tau) \frac{\partial^2 u_t}{\partial x \partial \tau} d\tau \qquad (25)$$

Inserting now the constitutive relations (23) and (25) in the equations of motion (22) one gets:

$$\frac{\partial^2 u_i}{\partial t^2} = \frac{E_1}{\rho_1}\frac{\partial^2 u_i}{\partial x^2} = C_1^2\frac{\partial^2 u_i}{\partial x^2}$$

$$\frac{\partial^2 u_r}{\partial t^2} = \frac{E_1}{\rho_1}\frac{\partial^2 u_r}{\partial x^2} = C_1^2\frac{\partial^2 u_r}{\partial x^2} \qquad (26)$$

$$\frac{\partial^2 u_t}{\partial t^2} = \frac{1}{\rho_2}\frac{\partial}{\partial x}\int_{0^+}^{t} E_2(t-\tau)\frac{\partial^2 u_t}{\partial x\partial\tau}\,d\tau = \frac{1}{\rho_2}\int_{0^+}^{t} E_2(t-\tau)\frac{\partial^3 u_t}{\partial x^2\partial\tau}\,d\tau$$

Here C_1 is the pulse velocity in the elastic bar which is known to be equal to $\sqrt{E_1/\rho_1}$. Equations (26) will now be solved by means of a Laplace transform technique. Taking the Laplace transform of the second equation in (26) and denoting by p the transform variable, and by $\bar{u}_r$ the transformed reflected displacement, one gets:

$$p^2\bar{u}_r = C_1^2\frac{\partial^2\bar{u}_r}{\partial x^2}$$

or:

$$\frac{\partial^2\bar{u}_r}{\partial x^2} - \frac{p^2}{C_1^2}\bar{u}_r = 0 \qquad (27)$$

Taking now the Laplace transform of the third equation in (26) and denoting by $\bar{u}_t$ the transformed transmitted displacement and by $\bar{E}_2$ the transformed stress relaxation function, one gets:

$$p^2\bar{u}_t = \frac{1}{\rho_2}\bar{E}_2 p\frac{\partial^2\bar{u}_t}{\partial x^2}$$

or:

$$\frac{\partial^2 \bar{u}_t}{\partial x^2} - \frac{\rho_2}{\bar{E}_2} p\bar{u}_t = 0 \tag{28}$$

In the derivation of equations (27) and (28), zero initial condition were assumed, which is in accordance with the assumption already stated that all pulses are considered to be smooth functions of time.

Equations (27) and (28) can now be solved for the displacements $\bar{u}_r$ and $\bar{u}_t$ thus yielding:

$$\begin{aligned} \bar{u}_r &= A_1 e^{\frac{p}{C_1} x} + A_2 e^{-\frac{p}{C_1} x} \\ \bar{u}_t &= B_1 e^{\sqrt{\frac{\rho_2}{\bar{E}_2}} p\, x} + B_2 e^{-\sqrt{\frac{\rho_2}{\bar{E}_2}} p\, x} \end{aligned} \tag{29}$$

Assuming the two bars to be very long, we must have:

$$A_2 = B_1 = 0$$

The condition $A_2 = 0$ is necessary in order to prevent an infinite growth of the reflected pulse on its travel in the negative x direction. The condition $B_1 = 0$ is necessary in order to prevent an infinite growth of the transmitted pulse on its travel in the positive x direction. Thus, expressions (29) may be reduced to:

$$\bar{u}_r = A_1 e^{\frac{p}{C_1} x}$$

$$\bar{u}_t = B_2 e^{-\sqrt{\frac{\rho_2}{\bar{E}_2}}\, p\, x} \tag{30}$$

The two constants A_1 and B_2 might be found from the boundary conditions at x=0. Those conditions require the equality of displacements and stresses across the boundary, and therefore may be written as:

$$\begin{aligned} &(a) \quad \bar{u}_i + \bar{u}_r = \bar{u}_t \\ &\qquad\qquad\qquad\qquad \text{at} \quad x=0 \\ &(b) \quad \bar{\sigma}_i + \bar{\sigma}_r = \bar{\sigma}_t \end{aligned} \tag{31}$$

Here $\bar{\sigma}_i$, $\bar{\sigma}_r$ and $\bar{\sigma}_t$ denote transformed stresses. Expressing now the constitutive relations (23) and (25) in terms of their Laplace transforms we get:

$$\begin{aligned} \bar{\sigma}_i &= E_1 \frac{\partial \bar{u}_i}{\partial x} \\ \bar{\sigma}_r &= E_1 \frac{\partial \bar{u}_r}{\partial x} \\ \bar{\sigma}_t &= \bar{E}\, p\, \frac{\partial \bar{u}_t}{\partial x} \end{aligned} \tag{32}$$

Inserting the last expressions for the transformed stresses in the second boundary condition (31b) one gets:

$$E_1\left(\frac{\partial \bar{u}_i}{\partial x} + \frac{\partial \bar{u}_r}{\partial x}\right) = \bar{E}_2 p \frac{\partial \bar{u}_t}{\partial x} \quad \text{at} \quad x=0 \tag{31c}$$

Rewriting now the boundary conditions (31a) and (31c) in a slightly different form we get:

$$\bar{u}_t - \bar{u}_r = \bar{u}_i$$
$$\frac{\bar{E}_2}{E_1} p \frac{\partial \bar{u}_t}{\partial x} - \frac{\partial \bar{u}_r}{\partial x} = \frac{\partial \bar{u}_i}{\partial x} \qquad \text{at} \quad x=0 \qquad (33)$$

Now, since the incident pulse is propagating in the elastic bar, we know that it has to be expressed in the form:

$$u_i(x,t) = u_i(t - \frac{x}{C_1})$$

Taking the Laplace transform of both sides we get:

$$\bar{u}_i = e^{-\frac{x}{C_1} p} \bar{u}_i(p) \qquad (34)$$

where $\bar{u}_i(p)$ is the transform of the displacement shape $u_i(t)$.

Differentiating expression (34) w.r.t. x, we also get:

$$\frac{\partial \bar{u}_i}{\partial x} = - \frac{p}{C_1} e^{-\frac{x}{C_1} p} \bar{u}_i(p) \qquad (35)$$

Before using the boundary conditions (33) we also need to find expressions for $\frac{\partial \bar{u}_r}{\partial x}$ and $\frac{\partial \bar{u}_t}{\partial x}$.

These may be found by differentiating w.r.t x the displacements in expression (30), thus yielding:

$$\frac{\partial \bar{u}_r}{\partial x} = \frac{p}{C_1} A_1 e^{\frac{p}{C_1} x} \qquad (36a)$$

$$\frac{\partial \bar{u}_t}{\partial x} = -\sqrt{\frac{\rho_2}{\bar{E}_2}p}\, B_2 e^{-\sqrt{\frac{\rho_2}{\bar{E}_2}p}\, x} \qquad (36b)$$

Now we can substitute expressions (30), (34), (35) and (36) in the boundary conditions (33), thus getting (at x=0):

$$\begin{aligned} B_2 - A_1 &= \bar{u}_j(p) \\ -\frac{\bar{E}_2}{E_1}\, p \sqrt{\frac{\rho_2}{\bar{E}_2}p}\, B_2 - \frac{p}{C_1} A_1 &= -\frac{p}{C_1}\, \bar{u}_i(p) \end{aligned} \qquad (37)$$

Solving the last two equations for the constants A_1 and B_2, and substituting $\rho_1 C_1^2$ for E_1, one gets:

$$\begin{aligned} A_1 &= \frac{\rho_1 C_1 - \sqrt{\rho_2 \bar{E}_2}\, p^{1/2}}{\rho_1 C_1 + \sqrt{\rho_2 \bar{E}_2}\, p^{1/2}}\, \bar{u}_i(p) \\ B_2 &= \frac{2\rho_1 C_1}{\rho_1 C_1 + \sqrt{\rho_2 \bar{E}_2}\, p^{1/2}}\, \bar{u}_i(p) \end{aligned} \qquad (38)$$

Inserting the constants A_1 and B_2 from expressions (38) in expression (30) for the transformed displacements, one gets:

$$\begin{aligned} \text{(a)} \quad \bar{u}_r &= e^{\frac{p}{C_1}x}\, \frac{\rho_1 C_1 - \sqrt{\rho_2 \bar{E}_2}\, p^{1/2}}{\rho_1 C_1 + \sqrt{\rho_2 \bar{E}_2}\, p^{1/2}}\, \bar{u}_i(p) \\ \text{(b)} \quad \bar{u}_t &= e^{\sqrt{\frac{\rho_2}{\bar{E}_2}p}\, x}\, \frac{2\rho_1 C_1}{\rho_1 C_1 + \sqrt{\rho_2 \bar{E}_2}\, p^{1/2}}\, \bar{u}_i(p) \end{aligned} \qquad (39)$$

Expressions (39) give us the existing relations between the reflected and transmitted pulses and the incident pulse, in terms of transformed quantities.

Observing now that the reflected pulse is traveling in the elastic bar, it must have the following representation:

$$u_r(x,t) = u_r(t + \frac{x}{C_1})$$

Taking the Laplace transform of both sides we get:

$$\bar{u}_r = e^{\frac{x}{C_1}p}\ \bar{u}_r(p) \tag{40}$$

where $\bar{u}_r(p)$ is the transform of the displacement shape $u_r(t)$.

Inserting the last expression for $\bar{u}_r$ in the left-hand side of expression (39a), we get:

$$e^{\frac{x}{C_1}p}\ \bar{u}_r(p) = e^{\frac{p}{C_1}x}\ \frac{\rho_1 C_1 - \sqrt{\rho_2 \bar{E}_2}\ p^{1/2}}{\rho_1 C_1 + \sqrt{\rho_2 \bar{E}_2}\ p^{1/2}}\ \bar{u}_i(p)$$

or:

$$\frac{\bar{u}_r(p)}{\bar{u}_i(p)} = \frac{\rho_1 C_1 - \sqrt{\rho_2 \bar{E}_2}\ p^{1/2}}{\rho_1 C_1 + \sqrt{\rho_2 \bar{E}_2}\ p^{1/2}} \tag{41}$$

Expression (41) gives us the relation between the material properties in the elastic and viscoelastic bars and the transformed displacement shapes in the elastic bar. However, from an experimental point of view we are more interested in finding a relation similar to (41) which will involve strain shapes rather than displacement shapes. In order to do this let

us write again the expressions for the incident and reflected displacement pulses in the elastic bar:

$$u_i(x,t) = u_i(t - \frac{x}{C_1})$$

$$u_r(x,t) = u_r(t + \frac{x}{C_1})$$

Differentiating the last expressions once w.r.t. x and once w.r.t. t, we get:

$$\begin{aligned} \frac{\partial u_i}{\partial x} = \varepsilon_i &= -\frac{1}{C_1} u_i'(t - \frac{x}{C_1}) \\ \frac{\partial u_i}{\partial t} = v_i &= u_i'(t - \frac{x}{C_1}) \\ \frac{\partial u_r}{\partial x} = \varepsilon_r &= \frac{1}{C_1} u_r'(t + \frac{x}{C_1}) \\ \frac{\partial u_r}{\partial t} = v_r &= u_r'(t + \frac{x}{C_1}) \end{aligned} \qquad (42)$$

Here $\varepsilon_i, v_i, \varepsilon_r, v_r$ are the strains and particle velocities in the incident and reflected pulses.

From expressions (42) the following relations are obtained:

$$\begin{aligned} \frac{\partial u_i}{\partial t} &= -C_1 \varepsilon_i \\ \frac{\partial u_r}{\partial t} &= C_1 \varepsilon_r \end{aligned} \qquad (43)$$

Relations (43) will hold for any location x in the bar. If we now fix our attention to some arbitrary fixed point X in the bar, then the quantities $\frac{\partial u_i}{\partial t}$, ε_i, $\frac{\partial u_r}{\partial t}$, ε_r which appear in expressions (43) may be all considered as functions of time only at that fixed point X.

Hence we can integrate expressions (43) w.r.t. to time and get:

$$u_i(t) = -C_1 \int_0^t \varepsilon_i(t')dt'$$
$$u_r(t) = C_1 \int_0^t \varepsilon_r(t')dt' \qquad (44)$$

Taking now the Laplace transform of both sides of each one of the expressions in (44) we get:

$$\bar{u}_i(p) = -C_1 \frac{\bar{\varepsilon}_i(p)}{p}$$
$$\bar{u}_r(p) = C_1 \frac{\bar{\varepsilon}_r(p)}{p} \qquad (45)$$

Here $\bar{\varepsilon}_i(p)$ and $\bar{\varepsilon}_r(p)$ denote transformed strain shapes corresponding to $\varepsilon_i(t)$ and $\varepsilon_r(t)$. Inserting now the last expressions for $\bar{u}_i(p)$ and $\bar{u}_r(p)$ in expression (41), we get:

$$\frac{\bar{\varepsilon}_r(p)}{\bar{\varepsilon}_i(p)} = -\frac{\rho_1 C_1 - \sqrt{\rho_2 \bar{E}_2}\, p^{1/2}}{\rho_1 C_1 + \sqrt{\rho_2 \bar{E}_2}\, p^{1/2}} = \frac{\sqrt{\rho_2 \bar{E}_2}\, p^{1/2} - \rho_1 C_1}{\sqrt{\rho_2 \bar{E}_2}\, p^{1/2} + \rho_1 C_1} \qquad (46)$$

Expression (46) gives us the desired relations between the material properties in the elastic and viscoelastic bars and the transformed strain shapes in the elastic bar. It is worth noting that when the viscoelastic bar is replaced by an elastic bar, the stress relaxation function $E_2(t)$ turns out to be simply the constant Young's modulus E_2. In this case:

$$\bar{E}_2 = \frac{E_2}{p}$$

Inserting this value for $\bar{E}_2$ in expression (46) we get:

$$\frac{\bar{\varepsilon}_r(p)}{\bar{\varepsilon}_i(p)} = \frac{\sqrt{\rho_2 E_2} - \rho_1 C_1}{\sqrt{\rho_2 E_2} + \rho_1 C_1} = \frac{\rho_2 C_2 - \rho_1 C_1}{\rho_2 C_2 + \rho_1 C_1}$$

Taking the inverse Laplace transform of the last expression we get:

$$\frac{\varepsilon_r(t)}{\varepsilon_i(t)} = \frac{\rho_2 C_2 - \rho_1 C_1}{\rho_2 C_2 + \rho_1 C_1}$$

The last expression for $\frac{\varepsilon_r(t)}{\varepsilon_i(t)}$ is the same as the first relation in (5) which was obtained directly for the case of two elastic bars attached together. Returning to the problem of a visco-elastic bar attached to an elastic bar, we would like to have an explicit expression for $\bar{E}_2$ in terms of all the other related quantities which appear in our problem. This might be done with the aid of expression (46), yielding:

$$\bar{E}_2 = \frac{(\rho_1 C_1)^2}{\rho_2 p} \left(\frac{\bar{\varepsilon}_i + \bar{\varepsilon}_r}{\bar{\varepsilon}_i - \bar{\varepsilon}_r}\right)^2 \qquad (47)$$

If we now take the inverse Laplace transform of $\bar{E}_2$ which was found by using expression (47), the stress relaxation function $E_2(t)$ can be evaluated.

The necessary steps in the evaluation of $E_2(t)$ are therefore as follows:

First, the incident and reflected strain pulses $\varepsilon_i(t)$ and $\varepsilon_r(t)$ in the elastic bar are recorded graphically. Next, the transformed strains $\bar{\varepsilon}_i(p)$ and $\bar{\varepsilon}_r(p)$ are computed by using the regular Laplace transform formulas, namely:

$$\bar{\varepsilon}_i(p) = \int_0^\infty e^{-pt}\varepsilon_i(t)dt = \int_0^T e^{-pt}\varepsilon_i(t)dt$$
$$\bar{\varepsilon}_r(p) = \int_0^\infty e^{-pt}\varepsilon_r(t)dt = \int_0^T e^{-pt}\varepsilon_r(t)dt \qquad (48)$$

Here T is the duration of the two pulses, which accounts for the change in the upper limit of integration from ∞ to T. Since the strains $\varepsilon_i(t)$ and $\varepsilon_r(t)$ are not known in an analytic form, expressions (48) have to be evaluated numerically. This could be done for example by evaluating the integrals in (48) according to Simpson's rule using different values for p. In this way the values of $\bar{\varepsilon}_i(p)$ and $\bar{\varepsilon}_r(p)$ could be obtained for any chosen value of p. The next step will be to substitute the transformed strains $\bar{\varepsilon}_i(p)$ and $\bar{\varepsilon}_r(p)$ in expression (47), thus getting the value of $\bar{E}_2$ for any chosen value of p. The last step and certainly the most difficult one is to find $E_2(t)$ as an inverse Laplace transform of $\bar{E}_2$. We must observe in this respect, that finding the inverse Laplace transform of $\bar{E}_2$ would not be an easy task even if $\bar{E}_2$ would have been given in the form of an analytic expression in p. In our case the situation is even more complicated owing to the fact that $\bar{E}_2$ is given in the form of point values at different data points p, rather than in the form of an analytic function in the variable p.

Fortunately however, for most known viscoelastic materials, $E_2(t)$ does not change very rapidly w.r.t. time (see, for example, Ferry, Fig. 2-2 in p. 29). In such a case we can find the inverse Laplace transform by a very nice and simple approximate method developed by Schapery [8]. According to this method, $E_2(t)$ can be found from $\bar{E}_2$ by the following approximate formula:

$$E_2(t) \approx [p\bar{E}_2]_{p=\frac{0.5}{t}} \tag{49}$$

That is, $E_2(t)$ is found by multiplying the corresponding transformed function by the transform variable and evaluating the result at points p corresponding to points $\frac{0.5}{t}$.

Since the function $\bar{E}_2$ is given only for discrete data points p, also the result $E_2(t)$ will be calculated only for discrete time values t. Thus by finding $\bar{E}_2$ from the experimental values of $\varepsilon_i(t)$ and $\varepsilon_r(t)$ using expressions (48) and (47), and by later applying to it the approximate inversion formula (49), the stress relaxation function $E_2(t)$ may be evaluated for discrete time values t.

4. Experimental

4.1 Experimental Set-up

The experimental set-up which was used for the experiments described in this report is shown in Figs. 1a, 1b and 1c.

The oscilloscope shown in this set-up was a Tectronix dual-beam scope type 502A, and it had a polaroid camera attached to its screen. The triggering of the scope was done by the dropping ball, which upon hitting the upper bar, closed an electrical triggering circuit. The triggering circuit used is shown in Fig. 2.

When the upper bar was of a conducting material, it formed part of the triggering circuit. When the upper bar was an insulator, a thin layer of conducting paste was applied to the top face of the bar, thus enabling the dropping ball to close the triggering circuit upon hitting the edge of the bar.

The bars which were used in the experiments were in general 2 feet long and 1/2" in diameter. They were usually resting on the table, but sometimes suspended with the aid of 3 strings coming down from the ceiling. The dropping ball which was made of steel, was generally 1/2" in diameter.

The strain gages used in the experiments were paper base wire gages of the type SR-4, C-10 made by the BLH Company. These gages had a resistance of 1000Ω and gage factor of 3.0 and this made them capable of detecting very low strains of the order of magnitude of 10 $\frac{\mu\text{-in}}{\text{in}}$. Each of the strain gages which was used for measuring the transient strain pulses, was connected in a dynamic bridge circuit as shown in Fig. 3.

The input voltage E to this circuit, was produced by a set of 6V batteries joined in series. When a strain pulse passed through the measuring gage, the output voltage E_g was changed by the amount dE_g which was proportional to the strain ε. The voltage change dE_g was fed to the scope and recorded photographically by the camera. It is worth noting that conversion of the output voltage-change dE_g to strain units, although possible, was not in general necessary. The reason for this is that in the formulas which relate the material properties to the strain amplitudes, only strain ratios and not absolute strain values are involved. Since the strains are proportional to the corresponding output voltage-changes dE_g, their ratio is the same as the ratio of the corresponding voltage-changes. The measuring strain gages were bonded to the bars using either Eastman 910 adhesive or Duco cement. The strain gage in the upper bar was bonded at a distance of about $9\frac{1}{2}$" from the interface, and was thus capable of giving separate recordings of the incident and reflected pulses without any interference between them. The upper bar was always chosen to be elastic or very nearly so, and therefore there was no appreciable difference between strain pulses being recorded at the strain gage location, and the same pulses while traveling near the interface. This fact is important since in the formulas relating C_2 and tan δ' to the Fourier coefficients of the incident and reflected strain pulses, all coefficients involved are those belonging to strain pulses acting at the boundary x=0. Also, in the analysis which relates $E_2(t)$ to the

incident and reflected strain shapes, it was assumed from the beginning that the first bar was elastic. The other bar which could be either elastic or viscoelastic, had at least one strain gage mounted on it for recording the transmitted strain pulse. This recorded pulse, though not required for direct computations of material properties in the lower bar was used for additional information and as a check on the results. When the second bar was elastic, it was sufficient to glue to it one strain gage at any distance from the interface. Since no dispersion took place in this case, the recorded pulse had the same shape as it had while traveling near the interface or at any point in the bar. When the lower bar was viscoelastic, two strain gages were employed; one was mounted as close as possible to the interface, and the other was mounted at some distance from the interface. The first strain gage recorded the transmitted strain pulse near the interface, immediately after it had been generated, and the second strain gage recorded the same pulse after it had travelled some distance in this bar and had undergone considerable dispersion.

The dummy strain gages which were used in the dynamic bridge circuits, were bonded to a piece of metal and put in a closed metal box which provided the necessary shielding against external electrical noise. The attachment of the two bars was achieved either by applying a thin layer of grease between them and pressing them together using a short close-fit metal collar to insure their stability, or by gluing them together with Eastman 910 cement. Before such attachment was made, the two

edges to be connected were first machined on a lathe and then thoroughly lapped using a specially designed lapping tool. This lapping tool is shown diagramatically in Fig. 4.

The lapping operation was done by putting some compound paste between the metal block and the steel cylinder and rubbing the one against the other. In some cases it was found that a slight roughening of the bar edges was necessary in order to get better adhesion between the bars. In such cases, instead of compound paste, very fine emery paper was attached to the metal block, which in turn was rubbed against the steel cylinder as before. All the electrical wires in the experimental set-up (excluding the very short ones only) were shielded wires; this was done in order to prevent external electrical noise from interfering with the outputs of the strain gages.

4.2 Experimental Procedure

The bars which were used in the experiments were made of the following materials: Steel, aluminum, polystyrene, polyethylene, Lucite (p.m.m), green solid propellant (AVCO product), pinewood (direction of grain parallel to axis of bar), sandstone, compressed sand, and clay. (The densities of these materials are given in appendix II.)

Before the experimental procedure (which will later be described) was used with these bars, some preliminary experiments were conducted the object of which was to check various aspects of the overall experimental technique; these experiments will be described first.

The first preliminary experiment was to hit a single steel bar with a dropping ball and record the output of the strain-gage which was attached to it. The result of this experiment is shown in Fig. 5. The object of this experiment was to check the functioning of the overall experimental set-up, and to see what kind of a strain pulse was generated in the bar upon its being hit by the dropping ball.

The second preliminary experiment was done by joining together two similar steel bars, with the aid of grease and a short metal collar, and hitting the upper bar with a dropping ball. The outputs of the strain gages attached to both bars were recorded, and are shown in Fig. 6. The object of this experiment was to check whether or not good contact between two attached bars could be achieved by this means.

The next preliminary experiments were done by joining together an aluminum and a steel bar with a grease joint, and performing the same experiment, first with the aluminum bar on top, and then with the steel bar on top. The results of these experiments are shown in Figs. 7 and 8. The object of these experiments was to check the agreement between theory and experiment in the case of materials with known properties, and thus provide an additional verification of the adequacy of the experimental technique, to evaluate material properties of new materials.

Some additional preliminary experiments were then carried out with polystyrene bars, since it was decided to use a polystyrene bar as the upper bar in most of the experiments described

in this report. This choice was made since polystyrene is very close to being elastic, and its characteristic impedance does not differ greatly from the characteristic impedances of most of the other materials whose properties were being sought. This last consideration is important since the ratio between the characteristic impedances of the upper and lower bars must be such that while the amplitude of the reflected pulse should not be too small compared with that of the incident pulse, it should also not be too close to it in magnitude.

Thus if the reflected strain pulse be too small, it will be difficult to distinguish it from the small disturbances which are present in the tail of the incident pulse. If on the other hand, the reflected pulse has almost the same amplitude (in absolute value) as the incident pulse, large errors may appear in the computations of the material properties of the lower bar.

The reason for this is that these computations are largely dependent on the arithmetic difference between the absolute values of the incident and reflected strain amplitudes. This could be shown for example by referring to expressions (5) which apply to the relatively simple case of two elastic bars attached together. From the first expression in (5) we get:

$$C_2 = \left(\frac{\varepsilon_1+\varepsilon_r}{\varepsilon_1-\varepsilon_r}\right)\left(\frac{\rho_1}{\rho_2}\right)C_1 \qquad (50)$$

Now, if both strains have the same sign, the difference between their absolute values appears in the denominator of the last

expression. If on the other hand, one strain has the opposite sign of the other, the difference between their absolute values will appear in the numerator of the last expression. At any rate, we see that the material property of the second bar, namely C_2, depends largely on the difference between the absolute values of ε_i and ε_r. If this difference is too small, any slight change in one of the strains will considerably effect the difference between the strains, and hence cause enormous errors in the computation of C_2. In some of the experiments described in this report, it was indeed necessary to choose for upper bars, steel or aluminum bars rather than polystyrene bars. This was done in order to get a better match between the characteristic impedance of the upper bar and that of the lower bar, according to the considerations discussed above.

Another reason for choosing most of the upper bars to be made of polystyrene rather than another glass-like plastic is, that a considerable amount of data is available on this material. The first experiment on polystyrene was to hit a single polystyrene bar with the dropping ball, and the result obtained is shown in Fig. 9. The objects of this experiment were: 1) to see what kind of a pulse is produced in these circumstances, 2) to determine the velocity of propagation of such a pulse in the bar, 3) to check how close the behavior of polystyrene approximated to perfect elasticity since, as mentioned above, it was necessary for the upper bar to be elastic or very close to it.

The second experiment on polystyrene was done with two polystyrene bars bonded with Eastman 910 cement. The top bar was hit by a dropping ball; the result of this experiment is shown in Fig. 10. The object of this experiment was to check whether or not it was possible to use cement as a means for attachment of the two bars without introducing appreciable errors in the experimental results.

Having described so far the preliminary experiments which were conducted on some of the bars, we will now describe the main experimental procedure which was applied to different bars in order to evaluate their material properties.

The first step in the procedure was to put an elastic or nearly elastic bar on top of the bar whose properties were being sought. When the lower bar was made of polyethylene, green solid propellant, wood, compressed sand, or clay, the upper bar was chosen to be a polystyrene bar. When the lower bar was made of Lucite, the upper bar was chosen to be an aluminum bar. When the lower bar was made of sandstone, the upper bar was chosen to be a steel bar.

The particular choice of the elastic bar in each case, was such that its characteristic impedance matched that of the lower bar, according to the considerations mentioned earlier in connection with the choice of polystyrene. The next step in the experimental procedure was to hit the upper bar with the dropping ball a number of times, and take the recordings from the different strain gages mounted on the bars, for different settings of amplification and beam sweep rate in the scope.

The results obtained in this way for different kinds of materials are all presented in Figs. 11 to 32. The last step in the experimental procedure was to take one of the pictures showing the incident and reflected strain pulses, project it on a sheet of paper attached to the wall and trace the magnified picture with a pencil. The magnified figures thus obtained could be analyzed according to the theory presented in the previous chapter. The results of such an analysis should have yielded the desired properties of the lower bar. However, as will be shown in the next chapter, the information which was obtained in this way was very limited owing to the large sensitivity of the calculated results to small changes in the pulse shape and the pulse starting time. Such changes may always be present as a result of small inaccuracies which are inherent in any experimental procedure.

4.3 Experimental Results

We may start with the result of the first preliminary experiment which is the picture shown in Fig. 5. This picture, which was obtained by hitting a single steel bar with the dropping ball, shows the same strain pulse travelling back and forth in the bar, and changing from compression to tension or vice versa, each time reflection takes place at one of the free edges of the bar. Similar pictures were obtained whether the bar was resting on the table, suspended vertically in the air, or suspended horizontally in the air and hit by a ball coming from the side.

The duration of the strain pulse shown in Fig. 5 is about 30 μsec. The second preliminary experiment which was done on two steel bars attached together, gave the picture shown in Fig. 6. In this picture the strain pulse in the upper beam is the incident strain, and the first pulse in the lower beam is the transmitted strain. The other pulses in the lower beam are the same transmitted strain being intermittently reflected from the bottom edge and the top edge of the lower bar.

Now, since the two bars in this experiment were made of the same material, if the contact was perfect it would be expected that the incident stress pulse which was travelling in the upper bar, would be entirely transmitted to the lower bar and no reflection should occur at the interface; that this indeed proved to be the case can be seen from Fig. 6.

From this figure we also note that the grease layer between the bars acted as a rectifier for stress pulses. It allowed the passage of a compression pulse from the upper bar to the lower bar, but prevented the passage of a tension pulse from the lower bar back to the upper bar. This of course is due to the ability of grease to transmit compression but yield in tension, causing the two bars to separate upon the arrival of a tension pulse at the interface. Such a tension pulse in the lower bar will therefore be reflected at the interface as a compression pulse in that bar, since the interface at that time acts as a free boundary. The results of the next preliminary experiments which were performed on an aluminum bar attached to

a steel bar, are shown in Figs. 7 and 8. Figure 7 was obtained with the aluminum bar on top, and Fig. 8 was obtained with the steel bar on top.

In both figures the incident and reflected pulses are shown in the upper beam and the transmitted pulse is shown in the lower beam. If the maximum amplitudes of those pulses are measured directly on the pictures, it is found that the relations between them (including the appropriate sign, which can be chosen as (+) for compression and (-) for tension, or vice versa) are in very good agreement with the theoretical relations given by expressions (5). This of course provides an additional verification of the adequacy of the experimental technique in evaluating material properties from strain measurements, for materials with unknown properties.

In Figures 7 and 8 we again see that after the reflected and transmitted strain pulses have been generated, the interface starts to act as a free boundary in each one of the bars, owing to the inability of the grease layer to sustain tension.

The next preliminary experiments which were performed on polystyrene bars, gave the results shown in Figs. 9 and 10. Figure 9 which was obtained by hitting a single polystyrene bar with the dropping ball is very similar to Fig. 5 which was obtained by performing the same experiment on a single steel bar. However there are some differences between the results of these two experiments. In the polystyrene bar experiment, the duration of the strain pulse is seen to be about 180 μsec whereas it is

only 30 μsec in the steel bar experiment. Also the strain amplitudes obtained in the polystyrene bar experiment, are very much higher than those obtained in the steel bar experiment. These differences are to be expected from the differences in Young's modulus between polystyrene and steel which result in corresponding differences in both duration and strain as given by Hertz's theory of indentation.

Another result which may be obtained from Fig. 9 is the pulse velocity in the polystyrene bar. This velocity can be calculated from the time it took the pulse to travel a fixed distance in the bar. By taking several measurements on Fig. 9, which correspond to different distances of travel, the velocity range in polystyrene was found to be 6000-6120 ft/sec. For practical purposes, a mean velocity of 6060 ft/sec. or 1850 m/sec. could be taken as the pulse velocity in polystyrene, that is:

$C_{polystyrene}$ = 6060 ft/sec. $\pm$ 1% = 1850 m/sec. $\pm$ 1%.

Another result which may be derived from Fig. 9 is that the attenuation of the pulse in the polystyrene bar is indeed very small. Hence, if a polystyrene bar is used as the upper bar in experiments which are done on materials like polyethylene or p.m.m., it can be considered to be elastic for all practical purposes. This was later verified by some additional computations which were done in connection with the derivation of material properties of polyethylene. These computations will be mentioned later.

The result of the second experiment with polystyrene, namely the one which was done on two polystyrene bars bonded together, is the picture shown in Fig. 10. From this picture we see that good contact between the two bars had been achieved, and the whole incident pulse was transmitted to the lower bar, just as in the case of the two attached steel bars. However, there is some difference between the two cases. In the steel bars experiment, the transmitted pulse could not travel back to the upper bar because the grease layer in the interface could not transmit tension pulses (this was explained before in detail). However in the polystyrene bars experiment, the transmitted pulse could travel back to the upper bar as can be seen from Fig. 10. The reason is that the cement in the interface could sustain tension as well as compression, and hence could transmit the tension pulse in the lower bar back to the upper bar.

Another conclusion which may be derived from the last experiment is, that the cement probably does not appear to interfere very much with the experimental results, and can therefore be safely used as a means for the attachment of one bar to another. Having presented so far the results of the preliminary experiments, we will now present the results of the main experiments, which for the sake of convenience will be described for each material separately.

Polyethylene

The results of a series of experiments in which polystyrene bars were attached to polyethylene bars, are shown in

Figs. 11, 12a, 12b, and 13. Figure 11 shows the incident and reflected strain pulses in the polystyrene bar (shown in the upper beam) and the transmitted strain pulse in the polyethylene bar (shown in the lower beam). Figures 12a and 12b, which were obtained from two similar experiments, give magnified pictures of the incident and reflected strain pulses. Figure 13 shows the transmitted strain pulse in the polyethylene bar; this pulse was recorded twice by the same strain gage, once while traveling away from the interface, and later while traveling back towards the interface after being reflected from the bottom edge of the bar.

Figures 12a and 12b must now be analyzed using the theory presented in chapter 3 in an attempt to evaluate the material properties of polyethylene. This was done by the use of computer programs, which included; 1) a sub-program for the evaluation of the Fourier coefficients of the incident and reflected strain pulses, 2) a sub-program for the evaluation of the Laplace transforms of the incident and reflected strain pulses. 3) Formulas for the evaluation of the desired material properties, that is, expressions (20) were used for the evaluation of tan δ' and C_2, and expressions (47) and (49) for the evaluation of $E_2(t)$.

In using these programs, a basic interval of 270 μsec (corresponding to a basic frequency of 3.7 kc/sec) was chosen for each one of the pulses in Figs. 12a and 12b. Each basic interval was divided into 75 divisions, and the corresponding pulse ordinates were read into the programs which were later run on the computer. It turned out however, that most of the results

obtained in this way were rather unreliable. In fact, when the ordinates of Fig. 12a were read into the computer program, tan δ' was obtained negative for all the Fourier harmonics. When the ordinates of Fig. 12b were put into the computer tan δ' was obtained positive for some Fourier harmonics (including the 1st harmonic), and negative for others, and it always differed very much from one harmonic to another. All these results are of course unacceptable, since it is known that tan δ' for polyehtylene is about 0.1 and is more or less constant over a wide range of frequencies. It was therefore suspected that small inaccuracies in the pulse shape and also in the location of the coordinate system used for the calculation of the Fourier coefficients, could cause enormous errors in the results of tan δ'. This indeed proved to be the case as will be shown in the next chapter. It is worth mentioning that the results of tan δ', ridiculous as they were, were not affected much by small variations in tan δ (δ is the phase angle in the polystyrene bar). In fact they were almost the same for tan δ between zero and 0.01 (the correct value of tan δ is less than 0.01). This verifies the assumption that polystyrene could be considered to be elastic for all practical purposes.

The results which were obtained for C_2 were quite reasonable for the first harmonic (the basic frequency), but again unreliable for the higher harmonics, the reasons being the same as those mentioned above in connection with the results of tan δ'.

The values of C_2 which were obtained for the basic frequency from Figs. 12a and 12b were 920 m/sec and 900 m/sec

respectively. (The values of C_2 which were obtained for the higher harmonics, were sometimes much above and sometimes much below these values. This is unacceptable since according to the linear theory of viscoelasticity, a linear increase of C_2 with the logarithm of the frequency would be expected when tan δ' is constant, and this is more or less so for polyetylene.)

It is interesting to compare these values with the value of C_2 which was obtained by Hillier [9] from direct experiments with polyethylene. Hillier's results were obtained for sinusoidal waves of different frequencies and at different room temperatures (see Ref.9, table 1, p. 705). The relevant part of Hillier's results is again presented in Appendix III for the convenience of the reader.

Interpolating Hillier's results for a frequency of 3.7 kc/sec (which was the basic frequency in all the previous calculations) and a temperature of 13°C (which was the temperature in the room when the experiments on polyethylene were performed), the resulting value for C_2 turns out to be 880 m/sec. This result is in good agreement with the results of C_2 previously obtained.

Another way of obtaining an approximate value for C_2 for the first harmonic from our experiments is to measure the distance between the pulse peaks in Fig. 13 and find the 'pulse velocity' in the same way as was done for the polystyrene bar. The location of the strain gage which gave the result shown in Fig. 13, was $6\frac{1}{8}$" from the bottom edge of the polyethylene bar. Since the distance between the pulse peaks is 5.6 cm on the

picture, and the sweep rate is 0.1 millisec/cm, the 'pulse velocity' turns out to be 870 m/sec. Now, in the case of an elastic bar, the value of the 'pulse velocity' is close to the value of the group velocity of the dominant frequency of its Fourier components. This group velocity is equal to $C-\Lambda \frac{dC}{d\Lambda}$, where C is the phase velocity and Λ is the wave length. When $\Lambda \frac{dC}{d\Lambda}$ is much smaller than C, the value of the group velocity is almost equal to the value of the phase velocity. Such a condition exists for example when the pulse length is much greater than the diameter of the bar, in which case the dispersion due to geometrical effects can be neglected. In the case of a viscoelastic bar, the above arguments are somewhat harder to justify since the concept of group velocity is not well defined. Nevertheless it seems reasonable to assume that in this case also, the 'pulse velocity' is still close to the phase velocity of the dominant Fourier harmonic, when $\Lambda \frac{dC}{d\Lambda}$ is much smaller than C. For such a condition to exist, $(\tan \delta)/\pi$ must be small compared with unity (the proof of this statement is given in Appendix IV). The geometrical dispersion must also be small as in the elastic case and this applies when the pulse length is much greater than the diameter of the bar. The conditions just mentioned were indeed valid for the pulse which was propagated in the polyethylene bar.

Hence, the value which was found for the 'pulse velocity' (870 m/sec) is probably very close to the value of the phase velocity C_2 for the first harmonic. Thus if the value of C_2 for the first harmonic is considered to be 870 m/sec to the first

approximation, we see that this value is in very good agreement with the values of C_2 previously obtained from the main theoretical analysis and from Hillier's results. Still another way of finding an approximate value for C_2 for the first harmonic from our experiments, is to measure the maximum strain amplitudes in Fig. 12a or Fig. 12b and use expression (50) for the evaluation of C_2.

Now, expression (50) was derived for two elastic bars attached together. However, as will be shown in the next chapter, the shape and amplitude of the reflected pulse will be almost the same whether the second bar is elastic or viscoelastic with small tan δ'. Hence the value of C_2 derived by using expression (50) and assuming that the two bars are elastic, is probably very close to the real value of C_2 for the first harmonic in the viscoelastic bar.

Evaluating C_2 for the first harmonic in this way from Fig. 12b (which is believed to be the more reliable figure between the two figures 12a and 12b), it is found that its value is 900 m/sec. This value of C_2 is in very good agreement with all the other values of C_2 previously obtained by different methods.

The results which were obtained for the stress relaxation function $E_2(t)$, by analyzing Figs. 12a and 12b according to the theory presented in the previous chapter, were rather unreliable, again due to the large effect of small experimental inaccuracies on the computed results. In fact, when Fig. 12a was used in order to calculate the values of $E_2(t)$, for different values of

time t, a monotonically increasing function w.r.t. time was obtained, which of course is physically unrealistic.

When small shifts were made in the location of the coordinate system of the reflected pulse (the coordinate system was used in order to calculate the Laplace transform of the pulse), different values for $E_2(t)$ were obtained, but the tendency to increase with time was still unchanged. When Fig. 12b (which has slightly different pulse shapes than those of Fig. 12a) was used in the calculations, $E_2(t)$ was obtained as a slightly decreasing function w.r.t. time. However, $E_2(t)$ could become an increasing function w.r.t time even in this case, if a small shift in the location of the coordinate system of the reflected pulse was made. Thus we see that the results for $E_2(t)$ were neither reproducible nor reliable. However the average value of $E_2(t)$ was very close to some effective dynamic Young's modulus E_{eff}, which can be set equal to $\rho_2 C_2^2$ where C_2 can be obtained by any one of the methods mentioned above. If the approximate value of C_2 is taken as 900 m/sec, the approximate value of E_{eff} for polyethylene turns out to be 7.9×10^3 kg/cm^2. A mathematical proof showing the large effects of small changes in coordinate location and pulse shapes on the function $E_2(t)$ is presented in the next chapter.

From the results obtained for polyethylene, we conclude that the only quantity which can be determined from the experiments with reasonable accuracy, is the phase velocity C_2 at the basic frequency p_o in the viscoelastic bar. However it was shown, that in order to find this phase velocity, there was no

need to use the rigorous analysis and go to the computer. Instead, direct measurements on Figs. 12 (either 12a or 12b) and 13, and straightforward calculations, result in a value of C_2 which is not less accurate than the value of C_2, which is obtained by the use of rigorous analysis. Thus, in order to find the phase velocity C_2 for materials other than polyethylene, only simple methods and straightforward calculations will be employed.

Lucite (p.m.m.)

The results of a series of experiments which were performed on aluminum bars attached to Lucite bars, are shown in Figs. 14, 15 and 16. Figure 14 shows the incident and reflected strain pulses in the aluminum bar (lower beam) and the transmitted strain pulse in the Lucite bar (upper beam). Figure 15 shows a magnified picture of the incident and reflected strain pulses in the aluminum bar. Figure 16 shows the transmitted pulse recorded by two strain gages bonded on the Lucite bar at a distance of $9\frac{1}{2}$" from each other. (The upper beam corresponds to the strain gage which was closer to the interface.) In order to find an approximate value for the phase velocity C_2 in the Lucite bar, the strain amplitudes in Fig. 15 were measured and inserted in expression (50). The value of C_2 thus obtained was 2150 m/sec. Another approximate value for C_2 was calculated from the time it took the transmitted pulse, shown in Fig. 16, to travel the distance between the two recording strain gages. The value of C_2 obtained in this way was 2070 m/sec.

The value of the correct phase velocity C_2 at the basic frequency p_o, is probably not very far from either one of the two values previously obtained, and hence could be taken approximately as 2100 m/sec. The value of the effective dynamic Young's modulus, based on the last value for C_2, turns out to be 5.3×10^4 kg/cm^2.

Green Solid Propellant (g.s.p.)

The results of a series of experiments done on a polystyrene bar attached to a g.s.p. bar are shown in Figs. 17, 18 and 19. Figure 17 shows the incident and reflected pulses in the polystyrene bar (lower beam) and the transmitted pulse in the g.s.p. bar (upper beam).

Figure 18 shows a magnified picture of the incident and reflected pulses in the polystyrene bar. Figure 19 shows the transmitted pulse twice recorded by the same strain gage which was located at a distance of 11" from the bottom edge of the g.s.p. bar.

The value of C_2 which was found from Fig. 18 by measuring the strain amplitudes and using expression (50), turned out to be 1080 m/sec.

The value of C_2 which was found from Fig. 19, by dividing the distance of travel of the transmitted pulse by the time of traverse, turned out to be 1050 m/sec. If the correct phase velocity for the first harmonic is assumed to have the value 1060 m/sec., the corresponding effective Young's modulus turns out to be 1.12×10^4 kg/cm^2.

Pine Wood

The results of a series of experiments which were carried out with a polystyrene bar attached to a pine wood bar are shown in Figs. 20, 21, and 22. The result of one experiment which was done by hitting a single pine wood bar with the dropping ball, is shown in Fig. 23.

Figure 20 shows the incident and reflected pulses in the polystyrene bar (upper beam), and the transmitted pulse in the wooden bar (lower beam). Figure 21 shows a magnified picture of the incident and reflected strain pulses. Figure 22 shows the transmitted pulse twice recorded by a strain gage which was located at a distance of $15\frac{3}{16}$" from the bottom edge of the wooden bar. Figure 23 shows one pulse traveling back and forth in a single pine wood bar. The values of C_2 which were found from Figs. 21 and 22 in the same way as for the g.s.p. bar, were 5550 m/sec and 5350 m/sec respectively. The value of C_2 which was found from Fig. 23 in the same way as was done in the single polystyrene bar was 5500 m/sec.

From Figs. 22 and 23 we see that the decay in the pulses traveling in the wooden bars was very small, and hence, wood can be considered as an elastic material for all practical purposes. If we assume that the correct value of the wave velocity in wood is 5500 m/sec., we get for Young's modulus (by writing $E=\rho C^2$) the value 2.16×10^5 kg/cm^2 which is in good agreement with the value of Young's modulus given in the literature for that kind of wood along the grain.

Sandstone

The results of a series of experiments with a steel bar attached to a sandstone bar, are shown in Figs. 24, 25 and 26.

Figure 24 shows the incident and reflected pulses in the steel bar (upper beam) and the transmitted pulse in the sandstone bar (lower beam). Figure 25 shows a magnified picture of the incident and reflected pulses in the steel bar. Figure 26 shows the transmitted pulse twice recorded by a strain gage which was located at a distance of $4\frac{13}{16}$" from the bottom edge of the sandstone bar.

The values of the phase velocity C_2 found from Figs. 25 and 26 by the same methods as before, are both 4100 m/sec. From Fig. 26 it can be seen that the decay in the sandstone is very small, and hence sandstone can be considered to be elastic for all practical purposes. The value of Young's modulus for sandstone turns out to be 4.63×10^5 kg/cm^2.

Clay

The results of a series of experiments performed on a polystyrene bar attached to a clay bar are shown in Figs. 27, 28 and 29. Figure 27 shows the incident and reflected strain pulses in the polystyrene bar (upper beam) and the transmitted pulse in the clay bar (lower beam). Figure 28 shows a magnified picture of the incident and reflected strain pulses. Figure 29 shows the transmitted pulse recorded by two strain gages attached to the clay bar. These strain gages were put 8 cm apart, and the distance between the lower gage and the bottom end of the clay bar was 10 cm. The upper beam in Fig. 29

corresponds to the upper gage, and the lower beam corresponds to the lower gage. The strain gages which were put on the clay bar, were pressed against the clay and held in position with a small piece of scotch tape. The outputs of these gages are probably far from giving the correct values of the strains in the clay, since the strain gages are much stiffer than the clay and therefore are not stretched to the same amount as the clay. Nevertheless, some useful information can still be obtained from the outputs of these gages, as will be shown later.

From Fig. 28, using expression (50), the phase velocity in clay is found to be 460 m/sec. Another value of C_2 is found by referring to Fig. 29 and dividing the distance between the two recording gages by the time it took the transmitted pulse to travel that distance. The value of C_2 found in this way is 470 m/sec.

The two values which were obtained for the wave velocity in clay are in good agreement with the value obtained by H. Calvit [10] which was 500 m/sec. The effective dynamic Young's modulus based on a phase velocity of 470 m/sec. turns out to be 4.05×10^3 kg/cm^2.

From Fig. 29 it can be seen that the decay of a strain pulse in clay is much larger than it is in the plastic materials previously mentioned. This conclusion is mainly based on the lower beam record which shows the transmitted pulse twice recorded by the same strain gage. Therefore, even if the pulses in the lower beam do not represent the true strains, the ratio between them is probably close to the ratio between the true

strains since they are both measured by the same strain gage.

Compressed Sand

The experiments with sand bars were done on wet sand bars and on dry sand bars. In both cases, the bars were prepared by pressing wet sand into hard paper tubes and later unwrapping these tubes. Some of the sand bars which were produced in this way, were put in a heated oven until they became dry.

The densities of the wet bars and the dry bars were found to be about the same. However the wet sand bars were much softer than the dry bars, and this had a considerable effect on the experimental results as shown below.

The results of a series of experiments done on polystyrene bars attached to wet sand bars are shown in Fig. 30. This figure shows the incident and reflected strain pulses in the polystyrene bar. By measuring the strain amplitudes on this figure and using expression (50), the wave velocity in wet sand is found to be 240 m/sec. The corresponding Young's modulus is found to be 1.23×10^3 kg/cm^2.

The results of a series of experiments done on polystyrene bars attached to dry sand bars, are shown in Figs. 31 and 32. Figure 31 shows the incident and reflected strain pulses in the polystyrene bar. Figure 32 shows the transmitted pulse in the sand bar being recorded by two strain gages which were carefully bonded to the bar at a distance of 3.5 cm apart.

From Fig. 31, and by using expression (50), the wave velocity in dry sand was found to be 470 m/sec. From Fig. 32,

by measuring the distance between the two pulse peaks, the wave velocity in dry sand was found to be 500 m/sec. (The strain gage outputs in Fig. 32 do not represent the true strains since the strain gages are much stiffer than the sand. However this fact does not affect the result which was obtained for the wave velocity.) The value of Young's modulus in dry sand corresponding to an average wave velocity of 480 m/sec. turns out to be 4.83×10^3 kg/cm^2.

From the results which were obtained for wet sand and for dry sand, we see that the wave velocity in dry sand was twice as large as that in wet sand, and Young's modulus in dry sand is four times larger than for wet sand. These differences in the dynamical behavior between dry sand and wet sand are in accordance with the differences observed between their stiffnesses when these materials are handled quasistatically.

5. Discussion of Results

5.1. General Remarks

In the previous chater it was mentioned, that the results which could be derived from the experiments by using the rigorous analysis presented in chapter 3, were very limited. The reason for this is that small changes in the location of the coordinate system in any of the pulses, as well as small changes in the shapes of the pulses, could cause enormous errors in the computations of the material properties of the lower bar. This is proved in the following sections.

5.2. Effect of Coordinate Shift on tan δ' and C_2

Let us consider an incident and reflected pulse as shown in Fig. 33. In this figure, the location of the origin of the reflected pulse which corresponds to the origin of the incident pulse, is not well defined. Hence we denote by 0 the true origin of the reflected pulse (corresponding to the ε_r, t coordinate system), and by 0' the erratic origin of this pulse (corresponding to the ε_r', t' coordinate system). The shift between the true and postulated coordinate systems is denoted by m, and it can have either a positive or a negative value.

If we now describe the incident pulse as a Fourier sum in its coordinate system, we have:

$$\varepsilon_i(t) = a_o + \sum_{k=1}^{\infty} a_{kc} \cos kp_o t + \sum_{k=1}^{\infty} a_{ks} \sin kp_o t$$

where:

$$a_o = \frac{1}{T}\int_o^T \varepsilon_i(t)dt$$

$$a_{kc} = \frac{2}{T}\int_o^T \varepsilon_i(t)\cos kp_o t\, dt$$

$$a_{ks} = \frac{2}{T}\int_o^T \varepsilon_i(t)\sin kp_o t\, dt$$

Describing now the reflected pulse in the postulated coordinate system (which we mistakingly consider to be the true coordinate system), we have:

$$\varepsilon_r'(t') = b_o' + \sum_{k=1}^{\infty} b_{kc}' \cos kp_o t + \sum_{k=1}^{\infty} b_{ks}' \sin kp_o t$$

where:

$$b_o' = \frac{1}{T}\int_o^T \varepsilon_r'(t')dt'$$

$$b_{kc}' = \frac{2}{T}\int_o^T \varepsilon_r'(t')\cos kp_o t'dt'$$

$$b_{ks}' = \frac{2}{T}\int_o^T \varepsilon_r'(t')\sin kp_o t'dt'$$

Describing the reflected pulse in its true coordinate system, we have

$$\varepsilon_r(t) = b_o + \sum_{k=1}^{\infty} b_{kc} \cos kp_o t + \sum_{k=1}^{\infty} b_{ks} \sin kp_o t$$

where:

$$b_o = \frac{1}{T}\int_o^T \varepsilon_r(t)dt$$

$$b_{kc} = \frac{2}{T}\int_o^T \varepsilon_r(t)\cos kp_o t\, dt$$

$$b_{ks} = \frac{2}{T}\int_o^T \varepsilon_r(t)\sin kp_o t\, dt$$

Since the reflected pulse is practically zero in the small regions near its edges, we can also write its true Fourier coefficients as follows:

$$b_o \simeq \frac{1}{T}\int_m^{T+m} \varepsilon_r(t)dt$$

$$b_{kc} \simeq \frac{2}{T}\int_m^{T+m} \varepsilon_r(t)\cos kp_o t\, dt$$

$$b_{ks} \simeq \frac{2}{T}\int_m^{T+m} \varepsilon_r(t)\sin kp_o t\, dt$$

Now, the relation between the mathematical descriptions of the reflected pulse in its two coordinate systems is:

$$\varepsilon_r(t) = \varepsilon_r'(t-m)$$

Hence, the true Fourier coefficients of the reflected pulse can be written as:

$$b_o = \frac{1}{T}\int_m^{T+m} \varepsilon_r'(t-m)dt$$

$$b_{kc} = \frac{2}{T}\int_m^{T+m} \varepsilon_r'(t-m)\cos kp_o t\, dt$$

$$b_{ks} = \frac{2}{T}\int_m^{T+m} \varepsilon_r'(t-m)\sin kp_o t\, dt$$

Substituting the relations $t-m = t'$ and $dt = dt'$ in the last integrals, and changing their limits accordingly, we get:

$$b_o = \frac{1}{T}\int_o^{T} \varepsilon_r'(t')dt'$$

$$b_{kc} = \frac{2}{T}\int_o^{T} \varepsilon_r'(t')\cos kp_o(t'+m)dt'$$

$$= \frac{2}{T}\int_o^{T} \varepsilon_r'(t')[\cos kp_o t' \cos kp_o m - \sin kp_o t' \sin kp_o m]dt'$$

$$b_{ks} = \frac{2}{T}\int_o^{T} \varepsilon_r'(t')\sin kp_o(t'+m)dt'$$

$$= \frac{2}{T}\int_o^{T} \varepsilon_r'(t')[\sin kp_o t' \cos kp_o m + \cos kp_o t' \sin kp_o m]dt'$$

Referring now back to the expressions for the Fourier coefficients of the postulated pulse we get from the last expression the following relations between the true and the postulated Fourier coefficients:

$$b_o = b_o'$$

$$b_{kc} = (\cos kp_o m)b_{kc}' - (\sin kp_o m)b_{ks}' \qquad (51)$$

$$b_{ks} = (\cos kp_o m)b_{ks}' + (\sin kp_o m)b_{kc}'$$

In order to demonstrate the effect of the shift "m" on the computations of tan δ' and C_2, we will assume for simplicity that the upper bar is perfectly elastic, that is tan $\delta = 0$. In this case tan δ' and C_2 are calculated from expressions (21). If we denote by (tan δ')' and C_2' the erratic properties corresponding to the postulated Fourier coefficients, and by tan δ' and C_2 the true properties corresponding to the true Fourier coefficients, we get from expressions (21) and (51) the following relations:

$$\text{(a)} \quad (\tan \delta') = \frac{-4(a_{kc}b_{ks}' - a_{ks}b_{kc}')}{a_{kc}^2 + a_{ks}^2 - b_{kc}'^2 - b_{ks}'^2}$$

$$\text{(b)} \quad C_2' = \left(\frac{\rho_1 C_1}{\rho_2}\right)\frac{(a_{kc}^2 + a_{ks}^2 - b_{kc}'^2 - b_{ks}'^2)}{(a_{kc}^2 + a_{ks}^2 + b_{kc}'^2 + b_{ks}'^2) - 2(a_{kc}b_{kc}' + a_{ks}b_{ks}')}$$

$$\text{(c)} \quad \tan \delta' = \frac{-4(a_{kc}b_{ks}' - a_{ks}b_{kc}')\cos kp_o m - 4(a_{kc}b_{kc}' + a_{ks}b_{ks}')\sin kp_o m}{a_{kc}^2 + a_{ks}^2 - b_{kc}'^2 - b_{ks}'^2}$$

$$\text{(d)} \quad C_2 = \left(\frac{\rho_1 C_1}{\rho_2}\right) \cdot \frac{(a_{kc}^2 + a_{ks}^2 - b_{kc}'^2 - b_{ks}'^2)}{(a_{kc}^2 + a_{ks}^2 + b_{kc}'^2 + b_{ks}'^2) - 2(a_{kc}b_{kc}' + a_{ks}b_{ks}')\cos kp_o m + 2(a_{kc}b_{ks}' - a_{ks}b_{kc}')\sin kp_o m} \qquad (52)$$

The ratios between the postulated and the true material properties will be:

$$\frac{(\tan\delta')'}{\tan\delta'} = \frac{a_{kc}b'_{ks}-a_{ks}b'_{kc}}{(a_{kc}b'_{ks}-a_{ks}b'_{kc})\cos kp_o m+(a_{kc}b'_{kc}+a_{ks}b'_{ks})\sin kp_o m}$$

$$\frac{C'_2}{C_2} = \tag{53}$$

$$\frac{(a_{kc}^2+a_{ks}^2+b_{kc}'^2+b_{ks}'^2)-2(a_{kc}b'_{kc}+a_{ks}b'_{ks})\cos kp_o m+2(a_{kc}b'_{ks}-a_{ks}b'_{kc})\sin kp_o m}{(a_{kc}^2+a_{ks}^2+b_{kc}'^2+b_{ks}'^2)-2(a_{kc}b'_{kc}+a_{ks}b'_{ks})}$$

If we assume for simplicity that the incident pulse is a symmetric pulse, then $a_{ks} \equiv 0$, and relations (53) reduce to:

$$\text{(a)}\quad \frac{(\tan\delta')'}{\tan\delta} = \frac{1}{\cos kp_o m + \frac{b'_{kc}}{b'_{ks}}\sin kp_o m}$$

$$\text{(b)}\quad \frac{C'_2}{C_2} = \tag{54}$$

$$\frac{(a_{kc}^2+b_{kc}'^2+b_{ks}'^2)-2(a_{kc}b'_{kc})\cos kp_o m + 2(a_{kc}b'_{ks})\sin kp_o m}{(a_{kc}^2+b_{kc}'^2+b_{ks}'^2) - 2(a_{kc}b'_{kc})}$$

Now, since the incident pulse was assumed to be symmetric, the reflected pulse will be very close to a symmetric pulse. The reason for this is, as will be shown later, that for small $\tan\delta'$, the reflected pulse has almost the same shape as the incident pulse. Hence, $b_{ks}'^2$ can be neglected in comparison to a_{kc}^2 and $b_{kc}'^2$, and expression (54b) becomes after some algebraic manipulations:

$$\frac{C'_2}{C_2} = 1 + 2\,\frac{a_{kc}(b'_{kc}\tan\frac{kp_o m}{2} + b'_{ks})}{(a_{kc}-b'_{kc})^2}\sin kp_o m \tag{54c}$$

From expression (54a) we see that $\frac{(\tan \delta')'}{\tan \delta'}$ is strongly dependent on the shift "m" even for small shifts. The reason is that the coefficient $\frac{b'_{kc}}{b'_{ks}}$ is very large (because b'_{ks} is very small in comparison to b'_{kc}, as was mentioned above), and hence the second term in the denominator of expression (54a) may become equal or larger (in absolute value) than the first term in the denominator of that expression.

If we assume that $\frac{b'_{kc}}{b'_{ks}}$ is positive, then for positive shifts m, $\frac{(\tan \delta')'}{\tan \delta'}$ may become much smaller than 1.0. For negative m, $\frac{(\tan \delta')'}{\tan \delta'}$ may become much larger than 1.0 which may cause very large errors in the value of tan δ'. In fact when m is negative, the whole denominator in (54a) may turn out to be negative, which leads to a negative $(\tan \delta')'$. Hence we see that relatively small shifts (of the order of 1% of the pulse width) may lead to absurd results for tan δ'.

From expression (54c) we see that $\frac{C'_2}{C_2}$ is moderately dependent on m. The reason is that the second term in the right hand side of expression (54c) is much smaller than 1.0 at least for the first few harmonics. Hence $\frac{C'_2}{C_2}$ is very close to 1.0 for the first few harmonics. However for the higher harmonics, $\tan \frac{kp_o m}{2}$ may become very large, causing large errors in $\frac{C'_2}{C_2}$. As will be shown later, the effect of small changes in the pulse shape may introduce large errors in C_2 even at the lower harmonics (with the exception of the first). Hence the only value of C_2 which can be obtained with reasonable accuracy is the value of C_2 for

the first harmonic. All the arguments which were presented till now, are still valid when the incident pulse has an arbitrary shape and not necessarily a symmetric one. In this case all the Fourier coefficients in expressions (53) must be taken into account, and the analysis becomes somewhat more involved. However, the conclusions which may be derived in this case are the same as those which were obtained for a symmetric incident pulse. In fact, when the pulses of Fig. 12b (which are all asymmetric) were used in the computations, the resulting values for tan δ' at the first harmonic varied between 0.6 and -0.5 for shifts between +2% and -2% of the pulse width (the true value for tan δ' in this case is 0.1). Similar or larger variations in tan δ' were also obtained for the higher harmonics. The resulting values for C_2 which were obtained from Fig. 12b varied between 890 m/sec and 910 m/sec. for the first harmonic (about 2% error) due to the shift effect.

The values of C_2 for the higher harmonics differed considerably from these values because of the shape effect which will be discussed later. However the deviations of C_2 at each harmonic from the mean value of C_2 at this harmonic, increased gradually from $\pm 1\%$ at the first harmonic to $\pm 50\%$ at the tenth harmonic due to shifts of $\pm 2\%$ of the pulse width.

5.3 Effect of Coordinate Shift on $E_2(t)$

Suppose that the incident and the reflected pulses are again those shown in Fig. 33. Now the stress relaxation function $E_2(t)$ may be computed from expressions (47) and (49) which yield

$$E_2(t) \simeq [p\bar{E}_2]_{p=\frac{0.5}{t}} = \frac{(\rho_1 C_1)^2}{\rho_2}\left[\left(\frac{\bar{\varepsilon}_i+\bar{\varepsilon}_r}{\bar{\varepsilon}_i-\bar{\varepsilon}_r}\right)^2\right]_{p=\frac{0.5}{t}} \qquad (55)$$

From a physical point of view, it is to be expected that $E_2(t)$ should be a slowly decreasing function w.r.t. time. Now, the time t is inversely proportional to the transform variable $p(p = \frac{0.5}{t})$. Thus $E_2(t)$ (or $p\bar{E}_2(p)$) must be a slowly increasing function w.r.t. p. We therefore conclude that the slope $\frac{d(p\bar{E}_2)}{dp}$ (or $\frac{dE_2(t)}{dp}$) must be positive and close to zero.

Suppose now that the origin of the reflected pulse was shifted a distance "m" from its exact location. The Laplace transform of the reflected pulse w.r.t. to its erratic coordinate system will be $e^{-mp}\bar{\varepsilon}_r$. Inserting this value of the transformed reflected pulse in expression (55), and denoting by $E_2'(t)$ the resulting erroneous stress relaxation function, we get:

$$E_2'(t) = \frac{(\rho_1 C_1)^2}{\rho_2}\left[\left(\frac{\bar{\varepsilon}_i+e^{-mp}\bar{\varepsilon}_r}{\bar{\varepsilon}_i-e^{-mp}\bar{\varepsilon}_r}\right)^2\right]_{p=\frac{0.5}{t}} \qquad (56)$$

Suppose now that the shift m is very small. In this case we can write approximately:

$$e^{-mp} \simeq 1 - mp$$

Substituting this value for e^{-mp} in expression (56), performing some algebraic manipulations and retaining only first order terms in m, we get:

$$E_2'(t) \simeq \frac{(\rho_1 C_1)^2}{\rho_2}\left[\left(\frac{\bar{\varepsilon}_i+\bar{\varepsilon}_r}{\bar{\varepsilon}_i-\bar{\varepsilon}_r}\right)^2 - 4mp\,\frac{\bar{\varepsilon}_i\bar{\varepsilon}_r(\bar{\varepsilon}_i+\bar{\varepsilon}_r)}{(\bar{\varepsilon}_i-\bar{\varepsilon}_r)^3}\right]_{p=\frac{0.5}{t}}$$

The erroneous slope $\frac{dE_2'(t)}{dp}$ will be:

$$\frac{dE_2'(t)}{dp} \simeq \frac{(\rho_1 C_1)^2}{\rho_2}\left\{\frac{d}{dp}\left(\frac{\bar{\varepsilon}_i+\bar{\varepsilon}_r}{\bar{\varepsilon}_i-\bar{\varepsilon}_r}\right)^2 - 4m\,\frac{d}{dp}\left[p\,\frac{\bar{\varepsilon}_i\bar{\varepsilon}_r(\bar{\varepsilon}+\bar{\varepsilon}_r)}{(\bar{\varepsilon}_i-\bar{\varepsilon}_r)^3}\right]\right\}$$

The first term in the right hand side of the last expression is simply the slope of the exact stress relaxation function $E_2(t)$. Thus we have:

$$\frac{dE_2'(t)}{dp} \simeq \frac{dE_2(t)}{dp} - 4m\,\frac{(\rho_1 C_1)^2}{\rho_2}\,\frac{d}{dp}\left[p\,\frac{\bar{\varepsilon}_i\bar{\varepsilon}_r(\bar{\varepsilon}_i+\bar{\varepsilon}_r)}{(\bar{\varepsilon}_i-\bar{\varepsilon}_r)^3}\right] \qquad (57)$$

Now, since $\frac{dE_2(t)}{dp}$ is small, the second term in the right hand side of expression (57) may be equal or larger (in absolute value) than the first term in that expression, even when "m" is very small. The second term may also have either positive or negative values depending on the sign of m, and the sign of $\frac{d}{dp}\left[p\,\frac{\bar{\varepsilon}_i\bar{\varepsilon}_r(\bar{\varepsilon}_i+\bar{\varepsilon}_r)}{(\bar{\varepsilon}_i-\bar{\varepsilon}_r)^3}\right]$. Hence $\frac{dE_2'(t)}{dp}$ may come out as many times larger or many times smaller than $\frac{dE_2(t)}{dp}$, or may even assume a negative value.

In fact, when $E_2(t)$ was computed from Fig. 12b, a slowly increasing function w.r.t. p (or slowly decreasing function w.r.t. t) was obtained for zero shift. However the slope of this function was tripled when a shift of +2% was introduced, and turned

negative when a shift of -2% was introduced (a negative slope means a decreasing function w.r.t. p or an increasing function w.r.t. t).

Thus we see that small errors in the location of the coordinate system in the reflected pulse, may introduce large errors in the slope of the stress relaxation function $E_2(t)$, and hence cause the curve of $E_2(t)$ vs. t to slope in the wrong direction.

5.4 Effect of Pulse Shape on tan δ' and C_2

In order to investigate the effect of small changes in the pulse shapes on tan δ', let us assume that two similar experiments gave exactly the same incident pulses but slightly different reflected pulses. We will again assume for simplicity that the incident pulses are symmetric (yielding $a_{ks} \equiv 0$) and hence the reflected pulses are very close to being symmetric. Denoting by the subscript (1) all the quantities which belong to the first reflected pulse, and by the subscript (2) all the quantities which belong to the second reflected pulse, we have from the first expression in (21):

$$\tan \delta'_{(1)} = - \frac{4a_{kc}b_{ks(1)}}{a_{kc}^2 - b_{kc(1)}^2 - b_{ks(1)}^2}$$

$$\tan \delta'_{(2)} = - \frac{4a_{kc}b_{ks(2)}}{a_{kc}^2 - b_{kc(2)}^2 - b_{ks(2)}^2}$$

Dividing $\tan \delta'_{(1)}$ by $\tan \delta'_{(2)}$ we get:

$$\frac{\tan \delta'_{(1)}}{\tan \delta'_{(2)}} = \left(\frac{a_{kc}^2 - b_{kc(2)}^2 - b_{ks(2)}^2}{a_{kc}^2 - b_{kc(1)}^2 - b_{ks(1)}^2}\right)\left(\frac{b_{ks(1)}}{b_{ks(2)}}\right) \qquad (58)$$

Now $b_{ks(1)}$ and $b_{ks(2)}$ are both very small quantities in comparison to all the other Fourier coefficients (for $\tan \delta' = 0$ we will get an exactly symmetric reflected pulse, and hence $b_{ks} = 0$). However the ratio between them may be much larger than unity or much smaller than unity or even negative.

Hence we see that small changes in the pulse shape may lead to completely different results for $\tan \delta'$. In order to illustrate all the above considerations, let us assume that the incident pulse has the form of a half sine wave in the interval $0-\pi$, and the reflected pulses will then have the form of a slightly asymmetric half sine wave in the same interval.

The suitable expressions for all these pulses may be written as:

$$\varepsilon_i = A \sin t$$

$$\varepsilon_{r(1)} = Be^{\alpha_1 t} \sin t$$

$$\varepsilon_{r(2)} = Be^{\alpha_2 t} \sin t$$

Here α_1 and α_2 are small numbers and determine the location of the pulse peak (which is very close to $\pi/2$).

Computing the Fourier coefficients of all three pulses and neglecting α^2 w.r.t. unity we get:

$$a_{kc} = -\frac{4A}{\pi}\frac{1}{4k^2-1}$$

$$b_{kc(1)} = -\frac{2(e^{\alpha_1\pi}+1)}{\pi}\frac{B}{4k^2-1}$$

$$b_{kc(2)} = -\frac{2(e^{\alpha_2\pi}+1)}{\pi}\frac{B}{4k^2-1}$$

$$b_{ks(1)} = -\frac{8\alpha_1(e^{\alpha_1\pi}+1)}{\pi}\frac{kB}{(4k^2-1)^2}$$

$$b_{ks(2)} = -\frac{8\alpha_2(e^{\alpha_2\pi}+1)}{\pi}\frac{kB}{(4k^2-1)^2}$$

Since α_1 and α_2 are small numbers (say 0.04 and 0.02) we get:

$$b_{kc(1)} \simeq b_{kc(2)} \simeq -\frac{4B}{\pi}\frac{1}{4k^2-1}$$

$$b_{ks(1)} \simeq -\frac{16\alpha_1}{\pi}\frac{kB}{(4k^2-1)^2}$$

$$b_{ks(2)} \simeq -\frac{16\alpha_2}{\pi}\frac{kB}{(4k^2-1)^2}$$

Thus, from expression (58) and by neglecting $b^2_{ks(1)}$ and $b^2_{ks(2)}$ w.r.t. all the other Fourier coefficients, we get:

$$\frac{\tan\delta'_{(1)}}{\tan\delta'_{(2)}} \simeq \frac{\alpha_1}{\alpha_2}$$

Now α_1 can be two or three times larger than α_2 or even have the opposite sign of α_2. Hence $\tan\delta'_{(1)}$ may differ considerably from $\tan\delta'_{(2)}$ and this results from just small changes in the shape of the reflected pulse.

In order to investigate the effect of small changes in the pulse shapes on C_2, let us assume now that two similar experiments result in the same reflected pulses but from two slightly different incident pulses which had the same maximum amplitudes. We will again assume for simplicity that the incident pulses are symmetric. Denoting by the subscript (1) all the quantities belonging to the first incident pulse, and by the subscript (2) all the quantities which belong to the second incident pulse, we get from the second expression in (21):

$$C_{2(1)} = \left(\frac{\rho_1 C_1}{\rho_2}\right) \frac{a_{kc(1)}^2 - b_{kc}^2 - b_{ks}^2}{(a_{kc(1)} - b_{kc})^2 + b_{ks}^2}$$

$$C_{2(2)} = \left(\frac{\rho_1 C_1}{\rho_2}\right) \frac{a_{kc(2)}^2 - b_{kc}^2 - b_{ks}^2}{(a_{kc(2)} - b_{kc})^2 + b_{ks}^2}$$

Dividing $C_{2(1)}$ by $C_{2(2)}$ and neglecting b_{ks}^2 in comparison to all the other Fourier coefficients, we get:

$$\frac{C_{2(1)}}{C_{2(2)}} \simeq \frac{\left(\frac{a_{kc(1)} + b_{kc}}{a_{kc(1)} - b_{kc}}\right)}{\left(\frac{a_{kc(2)} + b_{kc}}{a_{kc(2)} - b_{kc}}\right)} = \frac{(a_{kc(1)} + b_{kc})(a_{kc(2)} - b_{kc})}{(a_{kc(1)} - b_{kc})(a_{kc(2)} + b_{kc})} \qquad (59)$$

Now suppose that the first incident pulse is a half sine wave in the interval $0-\pi$, and the second incident pulse is a parabola in the same interval. Those two pulses, when plotted, are very similar to each other. The reflected pulse will be assumed as before to have the shape of a slightly asymmetric half sine wave.

The suitable expressions for all three pulses are:

$$\epsilon_{i(1)} = A \sin t$$

$$\epsilon_{i(2)} = \frac{4A}{\pi^2}(\pi t - t^2)$$

$$\epsilon_r = Be^{\alpha t} \sin t$$

The Fourier coefficients of the three pulses are:

$$a_{kc(1)} = -\frac{4A}{\pi}\frac{1}{4k^2-1}$$

$$a_{kc(2)} = -\frac{4A}{\pi^2}\frac{1}{k^2}$$

$$a_{ks(1)} = a_{ks(2)} = 0$$

$$b_{kc} = -\frac{2(e^{\alpha\pi}+1)}{\pi}\frac{B}{4k^2-1} \simeq -\frac{4B}{\pi}\frac{1}{4k^2-1} \quad \text{(for small } \alpha\text{)}$$

$$b_{ks} = -\frac{8\alpha(e^{\alpha\pi}+1)}{\pi}\frac{Bk}{(4k^2-1)^2} \simeq -\frac{16\alpha B}{\pi}\frac{k}{(4k^2-1)^2}$$

(for small α).

Substituting the Fourier coefficients in expression (59) we get:

$$\frac{C_{2(1)}}{C_{2(2)}} \simeq \frac{(\frac{4A}{\pi}\frac{1}{4k^2-1} + \frac{4B}{\pi}\frac{1}{4k^2-1})(\frac{4A}{\pi^2}\frac{1}{k^2} - \frac{4B}{\pi}\frac{1}{4k^2-1})}{(\frac{4A}{\pi}\frac{1}{4k^2-1} - \frac{4B}{\pi}\frac{1}{4k^2-1})(\frac{4A}{\pi^2}\frac{1}{k^2} + \frac{4B}{\pi}\frac{1}{4k^2-1})}$$

or

$$\frac{C_{2(1)}}{C_{2(2)}} \simeq \frac{(1+\frac{B}{A})(\frac{1}{\pi k^2} - \frac{B}{A}\frac{1}{4k^2-1})}{(1-\frac{B}{A})(\frac{1}{\pi k^2} + \frac{B}{A}\frac{1}{4k^2-1})}$$

Now let us suppose for example that the amplitude ratio B/A is equal to 0.5. Computing $C_{2(1)}/C_{2(2)}$ for the first three harmonics (k=1, k=2, k=3) we get:

$\frac{C_{2(1)}}{C_{2(2)}}$	k=1	k=2	k=3
	0.935	1.230	1.270

Thus we see that small changes in the shape of the incident pulse, though not effecting the value of C_2 at the first harmonic too much (7% error in our example), may introduce large errors in the values of C_2 at the higher harmonics (in our example we have 23% error in C_2 of the second harmonic and 27% error in C_2 of the third harmonic). The reason for the sensitivity of the value of C_2 (of the higher harmonics) to small changes in the pulse shape is, that the Fourier coefficients, excluding those of the first harmonic, are very dependent on the exact shape of the pulse. Thus, two pulses which have almost similar shapes, may have entirely different higher Fourier coefficients. The conclusions of the discussion presented up to now are quite general and will hold for pulses of arbitrary shape when subject to small changes in their shapes. When the pulses of Fig. 12b were analyzed, the resulting values for tan δ' for the first ten harmonics varied between -10 1 and 1.4 for a specific location of the coordinate syste in the reflected pulse.

(This location was the one which gave the correct result tan $\delta' = 0.1$ at the first harmonic. Other locations of the coordinate system resulted in even larger variations in tan δ'

computed for different harmonics.) The large variations in tan δ' are attributed mainly to small inaccuracies in the shapes of the pulses in Fig. 12b. These inaccuracies are probably introduced by small experimental errors. When the phase velocity C_2 was computed from Fig. 12b for the first ten harmonics, values between 600 m/sec. and 1770 m/sec. were obtained. (These values were obtained for the same location of the coordinate system which was mentioned before. For other locations of the coordinate system larger variations in C_2 were obtained.) The value which was obtained for C_2 for the first harmonic was 900 m/sec. which is probably close to the correct value for this harmonic. (A similar value for C_2 for the first harmonic was also obtained from Fig. 12a.)

From the discussion presented in this paragraph, we see that the computed values for tan δ' and C_2 (for the higher harmonics) are very sensitive to small changes in the pulse shape. The only quantity which is not effected too much by these small changes and hence could be computed with reasonable accuracy, is the phase velocity C_2 for the first harmonic.

5.5 Dependence of the Pulse Shape on tan δ'

In the previous paragraphs it was mentioned that for small tan δ', the shape of the reflected pulse is almost similar to the shape of the incident pulse (although the amplitudes are in general different.) A proof of this statement will now be given.

Before starting on this proof, however, we need to know the relations between the Fourier coefficients of the incident strain pulse and those of the reflected, strain pulse. This can be done by substituting relations (19) in the first two relations in (8) yielding (after some algebraic manipulations):

$$b_{kc} = -\left(\frac{1-s}{1+s}\right)a_{kc} + \frac{2s(\delta_2-\delta_1)}{(1+s)^2}\,a_{ks}$$
$$b_{ks} = -\left(\frac{1-s}{1+s}\right)a_{ks} - \frac{2s(\delta_2-\delta_1)}{(1+s)^2}\,a_{kc} \qquad (60)$$

Suppose now that the incident pulse is given in the basic interval $0-2\pi$ by:

$$\varepsilon_i = 0.0687e^{0.19(2.4-t)}t^{1.2}(2\pi-t)^{1.2}$$

This pulse is shown in Fig. 34. Suppose also that C_2 is changing with frequency as predicted by the linear theory of viscoelasticity for constant tan δ which yields:

$$C_2 \simeq C_{20}\left(1 + \frac{\tan\delta'}{\pi}\,\ell n\,\frac{p}{p_o}\right) \qquad (61)$$

Here C_{20} is the phase velocity at the basic frequency p_c. Our object now is to predict the shape of the reflected pulse for different values of tan δ', assuming that C_2 is varying with frequency according to expression (61). We will also assume for simplicity that the first bar is elastic. The first step is to find the Fourier coefficients of the incident pulse. From these coefficients, the corresponding Fourier coefficients of the reflected pulse may be found by using expressions (60) and (61).

(Expression (61) is used to compute "S" for each frequency.) From the Fourier coefficients of the reflected pulse, the shape of this pulse can be constructed.

The procedure just described was carried on with the aid of the computer, for two values of "S" at the basic frequency (0.5 and 0.75) and for five values of tan δ' (0, 0.05, 0.1, 0.2, 0.3). The results are shown in Figs. 35a, 35b, 35c, 35d. Figures 35a and 35c give the immediate results of the computations, from which it might appear (at least from Fig. 35c) that there are considerable differences between pulse shapes corresponding to different values of tan δ'. However a closer look at these figures reveals that in fact all the pulses are almost identical, and they are just shifted a small distance from each other. Thus, if all the pulses are shifted back towards each other, the results which are obtained are those shown in Figs. 35b and 35d. From Figs. 35b and 35d we see that any small value which is assumed for tan δ' results in almost the same reflected pulse. Thus it is again verified that tan δ' cannot be derived with sufficient accuracy from the strain pulses which were obtained in the experiments described in this report.

It is interesting to see from Figs. 35b and 35d that the reflected pulses for different values of tan δ', almost coincide with the reflected pulse for tan $\delta' = 0$ which corresponds to a perfectly elastic second bar. This provides some indication that the phase velocity for the first harmonic can be approximately computed by assuming that the two bars are elastic, and by

measuring the maximum amplitudes of the pulses and inserting them in expression (50) which in turn yields a straightforward result for C_2.

From expressions (5) which correspond to the case of two elastic bars attached together we have:

$$\varepsilon_r(t) = \left(\frac{\rho_2 C_2 - \rho_1 C_1}{\rho_2 C_2 + \rho_1 C_1}\right) \varepsilon_i(t)$$

Thus we see that in this case, the shapes of the incident and the reflected pulses are similar (although the amplitudes of the pulses are different). Now, since the shapes of the reflected pulses when $\tan \delta' \neq 0$ are very close to the shape of the reflected pulse when $\tan \delta' = 0$, we conclude that the reflected pulses are always close in shape to the incident pulse when $\tan \delta'$ is sufficiently small (say less than 0.3, which includes all the conventional plastics). The conclusions present in this paragraph are quite general and were also derived when different incident pulses were assumed.

5.6 Effect of Pulse Shape on $E_2(t)$

In order to investigate the effect of small changes in the pulse shape on $E_2(t)$ we will assume that $E_2(t)$ may be approximated to in a limited interval by:

$$E_2(t) = E_o e^{-\alpha t} \qquad (62)$$

For the time period 0-200 μsec (which is the approximate duration of most of the strain pulses obtained in the experiments), one may expect a reduction of about 5% in $E_2(t)$. For illustrative

purposes however, we will assume changes in $E_2(t)$ which will vary between 10% reduction and 5% increase. Thus we may write:

$$E_2(200) = E_o e^{-\alpha.200} = \beta E_o$$

where $0.90 \leq \beta \leq 1.05$.

From the last expression we get:

$$\alpha = -\frac{\ell n\ \beta}{200}$$

Hence:

$$\beta = 1.05 \rightarrow \alpha = -\ 2.439\times10^{-4}\ \mu sec^{-1}$$

$$\beta = 1.0 \rightarrow \alpha = 0$$

$$\beta = 0.9 \rightarrow \alpha = +5.268\times10^{-4}\ \mu sec^{-1}$$

The graphs $E_2(t)$ vs. t for these values of α are shown in Fig. 36. Now, assuming for $E_2(t)$ the form given in expression (62), we may use expression (46) in order to determine the relation between the shapes of the incident and the reflected strain pulses. Doing this we get:

$$\frac{\bar{\varepsilon}_r}{\bar{\varepsilon}_i} = \frac{\sqrt{\rho_2 \frac{E_o}{p+\alpha}}\ p - \rho_1 C_1}{\sqrt{\rho_2 \frac{E_o}{p+\alpha}}\ p + \rho_1 C_1} = \frac{\sqrt{\rho_2 \frac{E_o p}{p(1+\alpha/p)}} - \rho_1 C_1}{\sqrt{\rho_2 \frac{E_o p}{p(1+\alpha/p)}} + \rho_1 C_1} \quad (63)$$

Since α is very small, we may evaluate $\frac{1}{1+\frac{\alpha}{p}}$ as a Taylor series and retain only first order terms in α. Here we also assume that p is large compared with α so that $\frac{\alpha}{p}$ is still much less than unity. If p becomes small, which corresponds to t becoming large (recall $p = \frac{0.5}{t}$), the inaccuracy in the mathematical

procedure gradually increases. Evaluating $\frac{1}{1+\frac{\alpha}{p}}$ in a Taylor series and performing some other algebraic manipulations in (63), in which we only retain first order terms in α, we finally get:

$$\bar{\varepsilon}_r = \{\frac{\sqrt{\rho_2 E_o} - \rho_1 C_1}{\sqrt{\rho_2 E_o} + \rho_1 C_1} - \frac{\rho_1 C_1 \sqrt{\rho_2 E_o}}{(\sqrt{\rho_2 E_o} + \rho_1 C_1)^2} \frac{\alpha}{p}\} \bar{\varepsilon}_i$$

Taking the inverse Laplace transform of the last expression we get:

$$\varepsilon_r(t) = \frac{\sqrt{\rho_2 E_o} - \rho_1 C_1}{\sqrt{\rho_2 E_o} + \rho_1 C_1} \varepsilon_i(t) - \frac{\rho_1 C_1 \sqrt{\rho_2 E_o}}{(\sqrt{\rho_2 E_o} + \rho_1 C_1)^2} \alpha \int_o^t \varepsilon_i(\tau) d\tau \quad (64)$$

Expression (64) gives us the approximate relation between $\varepsilon_r(t)$ and $\varepsilon_i(t)$ for times which are not too large (say not larger than the pulse duration which is 200 μsec). In order to illustrate the dependence of $\varepsilon_r(t)$ on α, let us assume that $\varepsilon_i(t)$ is given as:

$$\varepsilon_i(t) = \begin{cases} \sin \frac{\pi t}{T_o} & 0 \leq t \leq T_o \\ 0 & t \geq T_o \end{cases}$$

Here T_o is the duration of the incident pulse which is assumed to be 200 μsec. Computing $\varepsilon_r(t)$ from expression (64) we get:

$$\varepsilon_r(t) = \begin{cases} \left(\frac{\sqrt{\rho_2 E_o} - \rho_1 C_1}{\sqrt{\rho_2 E_o} + \rho_1 C_1}\right) \sin \frac{\pi t}{T_o} - \frac{\rho_1 C_1 \sqrt{\rho_2 E_o}}{\left(\sqrt{\rho_2 E_o} + \rho_1 C_1\right)^2 \left(\frac{\pi}{T_o}\right)} \left(1 - \cos \frac{\pi t}{T_o}\right) \alpha & t \leq T_o \\ -\frac{2\alpha}{\left(\frac{\pi}{T_o}\right)} \frac{\rho_1 C_1 \sqrt{\rho_2 E_o}}{\left(\sqrt{\rho_2 E_o} + \rho_1 C_1\right)^2} & t \geq T_o \end{cases}$$

Assuming for example that $\frac{\sqrt{\rho_2 E_o}}{\rho_1 C_1} = 0.5$*, and plotting $\varepsilon_r(t)$ for the three values of α which were given above ($\alpha = -2.439 \times 10^{-4}$, $\alpha = 0$, $\alpha = +5.268 \times 10^{-4}$) we get the pulse shapes which are shown in Fig. 37a. From Fig. 37a it seems that there are some differences between the pulses $\varepsilon_r(t)$ which correspond to different values of α, especially near the tails of the pulses.

However, the mathematical treatment which results in Fig.37a is not accurate for large t, and in fact all the reflected pulses almost coincide also at the ends of their periods. This may be proved with the aid of a theorem, which relates the behavior of a function of t at $t \to \infty$ to the behavior of its Laplace transform when $p \to 0$. This theorem states:

$$\lim_{t \to \infty} \varepsilon_r(t) = \lim_{p \to o} p\, \bar{\varepsilon}_r$$

*If we define a characteristic pulse velocity C_2 in the second bar, such that $E_o = \rho_2 C_2^2$ then, $\frac{\sqrt{\rho_2 E_o}}{\rho_1 C_1} = \frac{\rho_2 C_2}{\rho_1 C_1}$ which is the ratio of some typical characteristic impedance in the second bar to the characteristic impedance of the first bar. A typical value for this ratio may be taken as 0.5.

Applying this theorem to expression (63) (which is valid for any value of α, p, and t) we get:

$$\lim_{t\to\infty} \varepsilon_r(t) = \lim_{p\to o} p\,\bar{\varepsilon}_r = \lim_{p\to o} p\,\bar{\varepsilon}_i \frac{\sqrt{\rho_2 \frac{E_o p}{p+\alpha}} - \rho_1 C_1}{\sqrt{\rho_2 \frac{E_o p}{p+\alpha}} + \rho_1 C_1} = 0 \quad (65)$$

The last is true because $\bar{\varepsilon}_i$ approaches a constant value when $p \to 0$. (In fact for $\varepsilon_i = \sin \frac{\pi t}{T_o}$ at $t \leq T_o$, we get

$$\bar{\varepsilon}_i = \frac{(\frac{\pi}{T_o})(1+e^{-pT_o})}{p^2 + (\frac{\pi}{T_o})^2} \quad \text{from which} \quad \lim_{p\to o} \bar{\varepsilon}_i = \frac{2}{(\frac{\pi}{T_o})} = \text{const.}$$

From (65) we see that all the reflected pulses for all values of α must approach zero when t is sufficiently large. Taking this last fact into account, it seems reasonable that all the reflected pulses will look like the pulses which are shown in Fig. 37b rather than those which are shown in Fig. 37a.

From Fig. 37b we see that for values of α between -2.439×10^{-4} μsec^{-1} and $+5.268\times10^{-4}$ μsec^{-1}, which corresponds to changes in $E_2(t)$ between a 5% increase and a 10% reduction, we get essentially the same reflected pulse. Thus we see that the graph of $E_2(t)$ versus t, cannot be derived with sufficient accuracy from the experimental results. In other words, very small changes in the shape of the reflected pulse may lead to large errors in the determination of the trend of the graph $E_2(t)$ versus t. However the average value of $E_2(t)$ in the limited interval of time 0-200 μsec, may be taken as the constant

value E_o corresponding to $\alpha=0$. This value was termed the effective dynamic Young's modulus in the previous chapter, and since it corresponds to a perfectly elastic second bar ($\alpha=0$ means $E_2(t)$ = const. which corresponds to an elastic material), it can be computed from the relation $E_2(t) = \rho C_2^2$ where C_2 is the pulse velocity in the second bar.

5.7 Concluding Remarks

It has been shown that most of the material properties of the second bar cannot be derived by the experimental technique described in this report.

This applies especially to tan δ' which should be derivable from the first expression in (21) (assuming that the first bar is perfectly elastic). The value which is computed from this expression is mainly governed by the numerator $a_{kc}b_{ks}-a_{ks}b_{kc}$. If both bars were elastic, the incident and the reflected pulses would have had exactly the same shapes so that $\varepsilon_r(t) = \lambda\varepsilon_i(t)$ where λ is some constant.

In this case:

$$b_{kc} = \lambda a_{kc}$$

$$b_{ks} = \lambda a_{ks}$$

and hence:

$$a_{kc}b_{ks}-a_{ks}b_{kc} = a_{kc}(\lambda a_{ks})-a_{ks}(\lambda a_{kc}) = 0.$$

Thus we see that in this case tan δ' turns out to be zero which was expected a priori.

However, when $\tan \delta' \neq 0$, the reflected pulse has a shape just slightly different from the shape of the incident pulse. In this case the difference $a_{kc}b_{ks}-a_{ks}b_{kc}$ is a very small number, and hence relatively small changes in any of the Fourier coefficients may considerably effect this difference, which in turn might result in enormous errors in the results for $\tan \delta'$. Now, changes in the Fourier coefficients may be caused by small errors in the zero of the coordinate system in the reflected pulse (see expressions (51)) or by small changes in the shapes of the pulses. Both effects are always present in any experiment because of inherent experimental errors.

The effects of small changes in the coordinate system location and small changes in the pulse shapes on C_2 and $E_2(t)$, are not so obvious at first sight as they are in the case of $\tan \delta'$. However some explanation and some examples were brought, which showed the large effect of small inaccuracies in the coordinate location and pulse shapes on C_2 and $E_2(t)$.

In the discussion given in this chapter, it was shown that the only quantity which may be determined from the experiments with reasonable accuracy is the phase velocity C_2 for the basic frequency p_o.

6. Summary

An experimental technique was described in this report from which theoretically, the material properties of viscoelastic materials could be derived. However from the experimental results and the discussion which followed, it was [redacted] the only quantity which could be determined with sufficient accuracy was the phase velocity at the basic frequency in the viscoelastic material. It was also shown that in order to determine approximately this phase velocity, there is no need to use a rigorous analysis. Instead, direct measurements and straightforward calculations based on elastic theory give the desired result with less effort and the same degree of accuracy.

Appendix I - Wave Propagation in Viscoelastic Bars

Consider an extensional wave traveling in the x direction along a thin viscoelastic bar. The equation of motion is:

$$\rho \frac{\partial^2 u}{\partial t^2} = \frac{\partial \sigma}{\partial x}$$

where u is the displacement in the x direction, ρ is the density of the bar and σ is the stress.

In order to solve this equation, we may try a solution of the form:

$$u = u_o e^{ip(t - \frac{x}{\bar{C}})}$$

This solution corresponds to a sinusoidal wave of angular frequency p traveling with phase velocity $\bar{C}$ along the bar in the direction of increasing x. From the expression for the displacement we get:

$$\sigma = (E_1 + iE_2) \frac{\partial u}{\partial x} = - \frac{ip}{\bar{C}} (E_1 + iE_2) u_o e^{ip(t - \frac{x}{\bar{C}})}$$

where $E_1 + iE_2$ is the complex Young's modulus of the material. Substituting the expressions for u and σ in the equation of motion, we get:

$$- \rho \frac{p^2}{\bar{C}^2} u_o e^{ip(t - \frac{x}{\bar{C}})} = - \frac{p^2}{\bar{C}^2} (E_1 + iE_2) u_o e^{ip(t - \frac{x}{\bar{C}})}$$

from which*

* We see that $\bar{C}$ turns out to be a complex phase velocity.

$$\bar{C}^2 = \frac{E_1+iE_2}{\rho} = \frac{\bar{E}e^{i\delta}}{\rho}$$

Here:

$$\bar{E} = \sqrt{E_1^2+E_2^2}$$

$$\tan \delta = E_2/E_1$$

Substituting the result for $\bar{C}$ in the expression for u, we get:

$$u = u_o e^{ip\left(t-\frac{x}{\sqrt{\bar{E}/\rho}\, e^{i\delta/2}}\right)} = u_o e^{ip\left[t-\frac{x(\cos\ \delta/2-i\ \sin\ \delta/2)}{\sqrt{\bar{E}/\rho}}\right]}$$

The last expression may be written as:

$$u = u_o e^{-\alpha x}\, e^{ip\left(t-\frac{x}{C}\right)}$$

where $C = \sqrt{\bar{E}/\rho}\ \sec\frac{\delta}{2}$ is the phase velocity of the wave and

$\alpha = \frac{p \tan\frac{\delta}{2}}{C}$ is the attentuation coefficient.

The above analysis also holds for a wave traveling in the direction of decreasing x, in which case we get:

$$u = u_o e^{+\alpha x}\, e^{ip\left(t+\frac{x}{C}\right)}.$$

Appendix II - Densities of the Materials Used in the Experiments

Material	Steel	Aluminum	Poly-styrene	Poly-ethylene	Lucite (p.m.m.)	G.S.P.	Pine Wood	Sand-stone	Compressed Sand	Clay
[gm/cm^3]	7.8	2.7	1.06	0.96	1.18	0.98	0.70	2.7	2.1	1.8

Appendix III - Hillier's Results for Phase Velocity in Polyethylene

Phase velocity [m/sec]

Temp. [°C]	Frequency [kc/sec]				
	1	2	5	10	16
0	1041	1066	1108	-	-
10	866	903	926	944	960
30	608	615	639	650	670
40	510	520	535	538	547

Appendix IV - Calculation of $\Lambda\frac{dC}{d\Lambda}$ for Viscoelastic Materials

The phase velocity in a linear viscoelastic material with a small tan δ, is dependent on the frequency according to the following relation (see Kolsky [11]):

(a) $$C = C_o(1 + \frac{\tan \delta}{\pi} \ln \frac{p}{p_o})$$

Here C is the phase velocity, p is the frequency, and C_o is the phase velocity at some reference frequency p_o. Now, since the frequency p is related to the phase velocity C and the wave length Λ by:

$$p = \frac{2\pi C}{\Lambda}$$

relation (a) can be written as:

(b) $$C = C_o(1 + \frac{\tan \delta}{\pi} \ln \frac{C}{C_o} \frac{\Lambda_o}{\Lambda})$$

Here Λ_o is the wave length at the reference frequency p_o. In order to calculate the value of $\Lambda\frac{dC}{d\Lambda}$, let us take the total differentials of both sides of expression (b):

$$dC = d[C_o + \frac{C_o \tan \delta}{\pi} \ln \frac{\Lambda_o}{C_o} + \frac{C_o \tan \delta}{\pi} (\ln C - \ln \Lambda)] =$$

$$= \frac{C_o \tan \delta}{\pi} \frac{dC}{C} - \frac{C_o \tan \delta}{\pi} \frac{d\Lambda}{\Lambda}$$

From the last expression we get:

$$dC(1 - \frac{\tan \delta}{\pi} \frac{C_o}{C}) = - \frac{C_o \tan \delta}{\pi} \frac{d\Lambda}{\Lambda}$$

Hence:

$$\Lambda\frac{dC}{d\Lambda} = -\frac{C_o \tan\delta}{\pi}\,\frac{1}{1-\frac{\tan\delta}{\pi}\frac{C_o}{C}}$$

For small tan δ, the ratio $\dfrac{\tan\delta}{1-\frac{\tan\delta}{\pi}\frac{C_o}{C}}$ can be expanded as a Taylor series in powers of tan δ. However if we retain only first order terms in tan δ, this ratio can be approximated by tan δ. Thus we have:

(c) $$\Lambda\frac{dC}{d\Lambda} \simeq -\frac{C_o \tan\delta}{\pi}$$

Now, from (a) and (c) the ratio between $\Lambda\frac{dC}{d\Lambda}$ and C is:

$$\frac{\Lambda\frac{dC}{d\Lambda}}{C} \simeq \frac{-C_o\frac{\tan\delta}{\pi}}{C_o(1+\frac{\tan\delta}{\pi}\ln\frac{p}{p_o})} = -\frac{\tan\delta}{\pi}\,\frac{1}{(1+\frac{\tan\delta}{\pi}\ln\frac{p}{p_o})}$$

For the first harmonic, this ratio has its maximum absolute value which is equal to $\frac{\tan\delta}{\pi}$. Thus, when $(\tan\delta)/\pi$ is small compared with unity, $\Lambda\frac{dC}{d\Lambda}$ is much smaller than C; for example, when tan δ is equal to 0.1, $\Lambda\frac{dC}{d\Lambda}$ is about 3% of the value of C.

Acknowledgements

The author wishes to thank his adviser, Professor H. Kolsky, for his kind assistance.

Thanks are also due to Professor R. Clifton for helpful suggestions, to Dr. J. Phillips for his help in laboratory experimentation, to Mr. L. Daubney and Mr. R. Stanton for their careful preparation of the specimans, and to Mrs. E. Fonseca for typing this report.

This report was done under a contract between the Army Research Office (Durham) and Brown University.

References

[1] B. Gross, "Mathematical Structure of the Theories of Viscoelasticity," Hermann, Paris, 1953.

[2] W. Flügge, "Viscoelasticity," Blaisdell, 1967.

[3] J.D. Ferry, "Viscoelastic Properties of Polymers," John Wiley & Sons, New York, 1961.

[4] D.R. Bland, "The Theory of Linear Viscoelasticity," Pergamon Press, London, 1960.

[5] H. Kolsky, "Stress Waves in Solids," Clarendon Press, Oxford, 1953; Dover Reprint, 1964.

[6] H. Kolsky, "Experimental Studies of the Mechanical Behavior of Linear Viscoelastic Solids," from "Proc. of the 4th Symp. on Naval Struc. Mech.," Pergamon Press, Oxford, New York, 1966.

[7] H. Kolsky and S.S. Lee, "The Propagation and Reflection of Stress Pulses in Linear Viscoelastic Media," Brown University Tech. Rept. No. 5, Contract Nonr 562(30), 1962.

[8] R.A. Schapery, "Approximate Methods of Transform Inversion for Viscoelastic Stress Analyses," Proc. 4th U.S. Nat. Cong. App. Mech., pp. 1075-1085, 1962.

[9] K.W. Hillier, "A Method of Measuring some Dynamic Elastic Constants and its Application to the Study of High Polymers," Proc. Phys. Soc., B62, p. 701, 1949.

[10] H.H. Calvit, D. Rader and J. Melville, "Some Wave-Propagation Experiments in Plasteline-clay Rods," Experimental Mechanics, p. 418, Sept. 1968.

[11] H. Kolsky, "The Propagation of Stress Pulses in Viscoelastic Solids," Phil. Mag., Vol. 1, p. 693, 1956.

Figure 1 - Experimental Set-Up

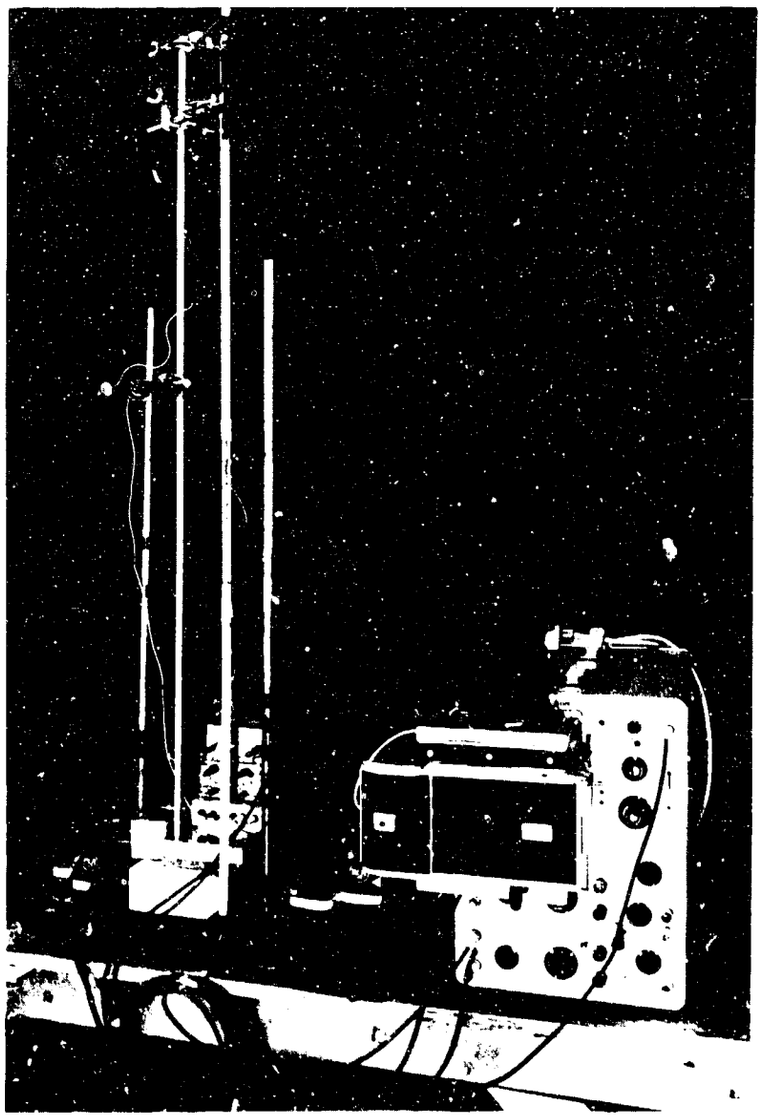

1a - General View of Set-Up.

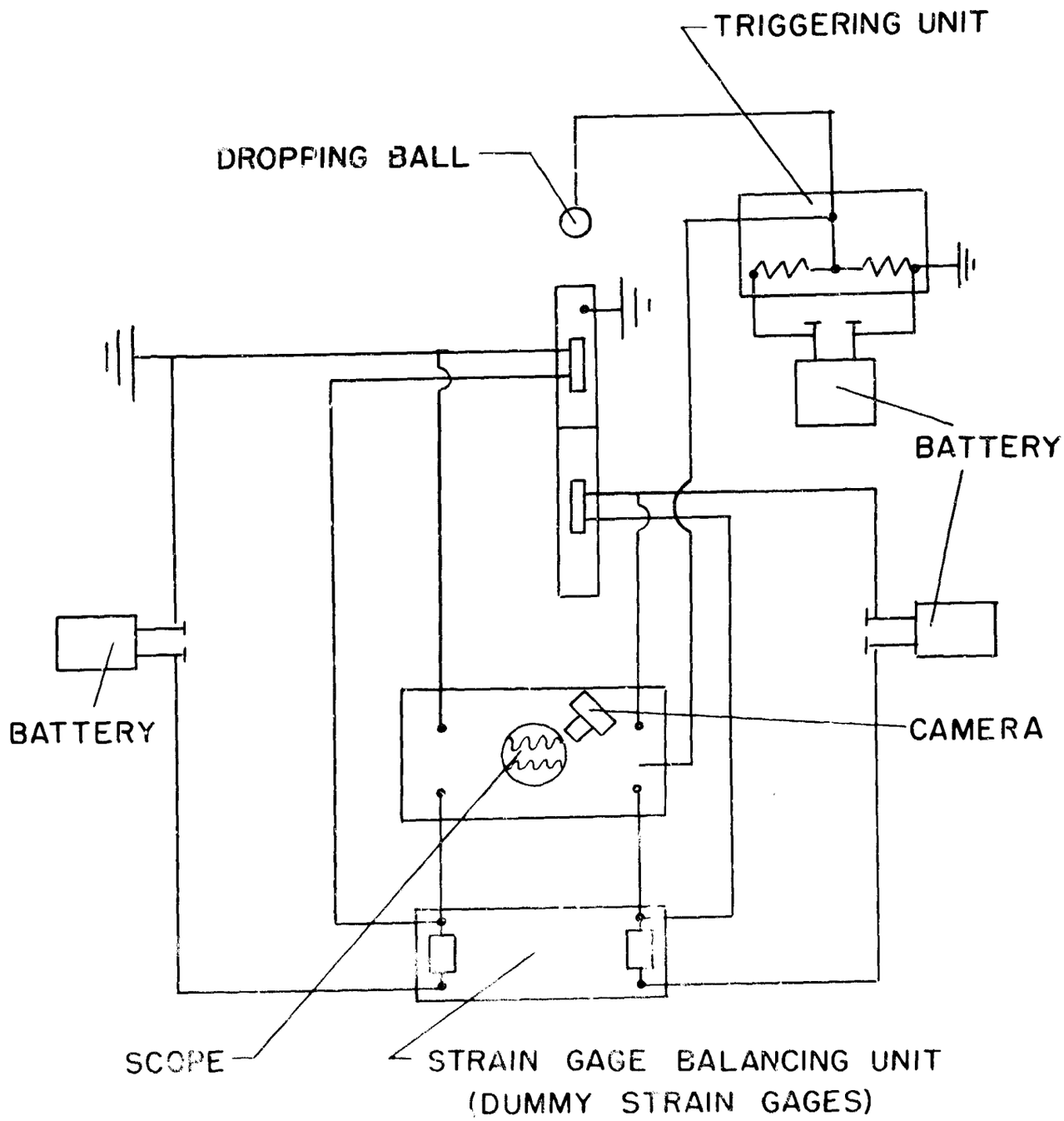

FIG 1b BLOCK DIAGRAM OF SET-UP

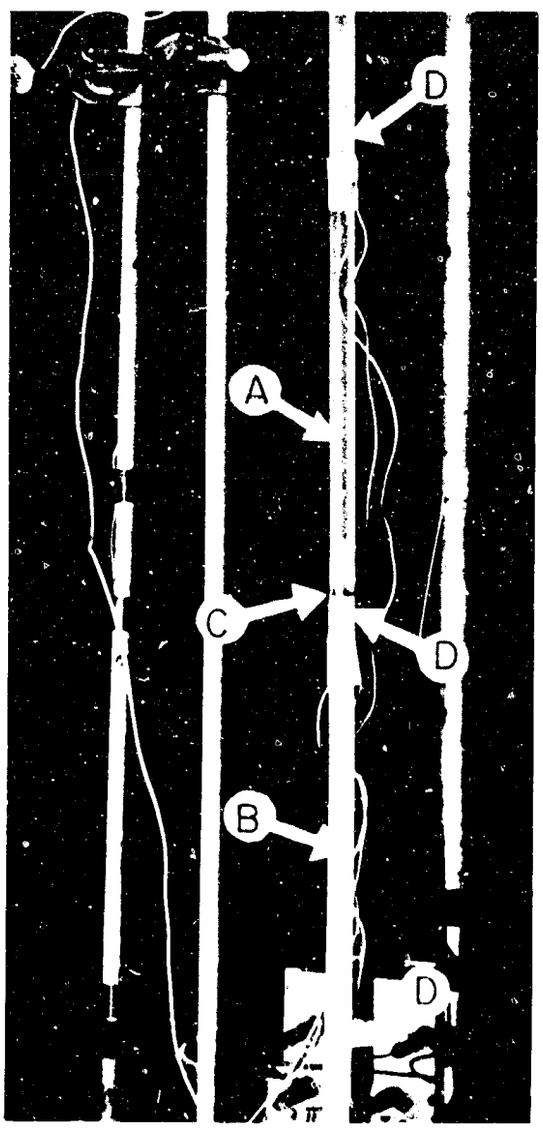

A - upper bar

B - lower bar

C - junction

D - strain gages

1c - Details of Junction Between Bars.

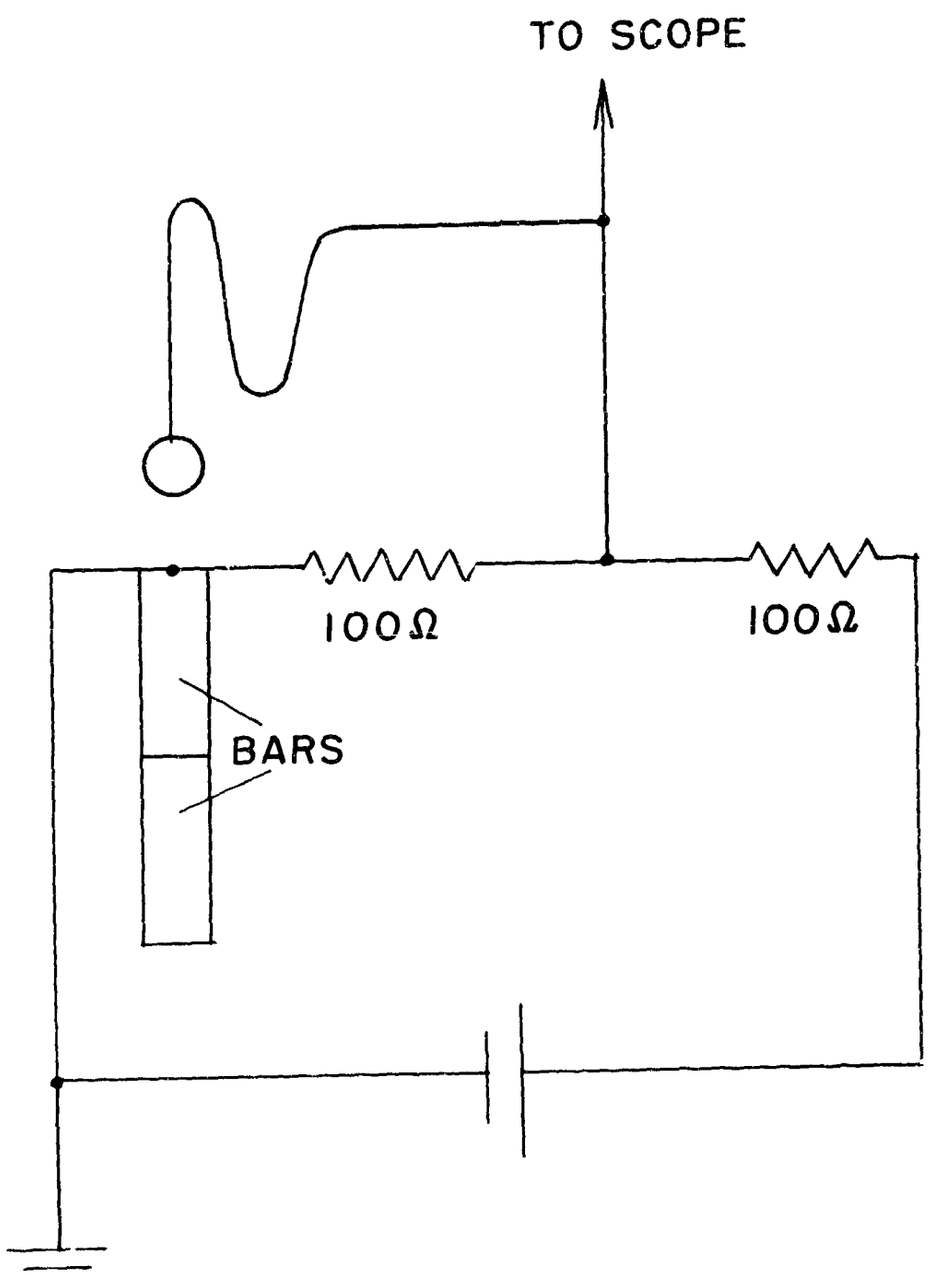

FIG. 2 TRIGGERING CIRCUIT

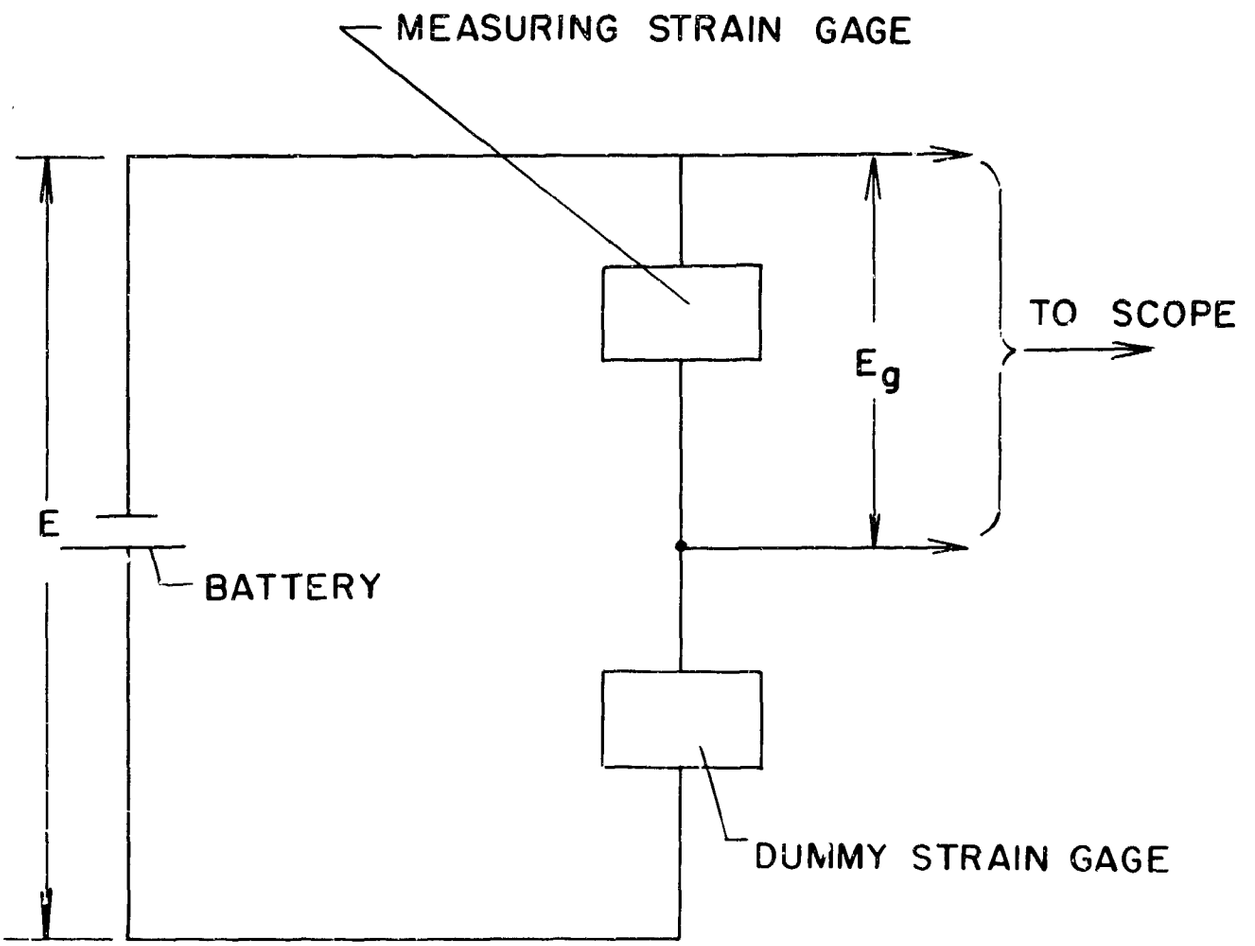

FIG. 3 DYNAMIC BRIDGE CIRCUIT

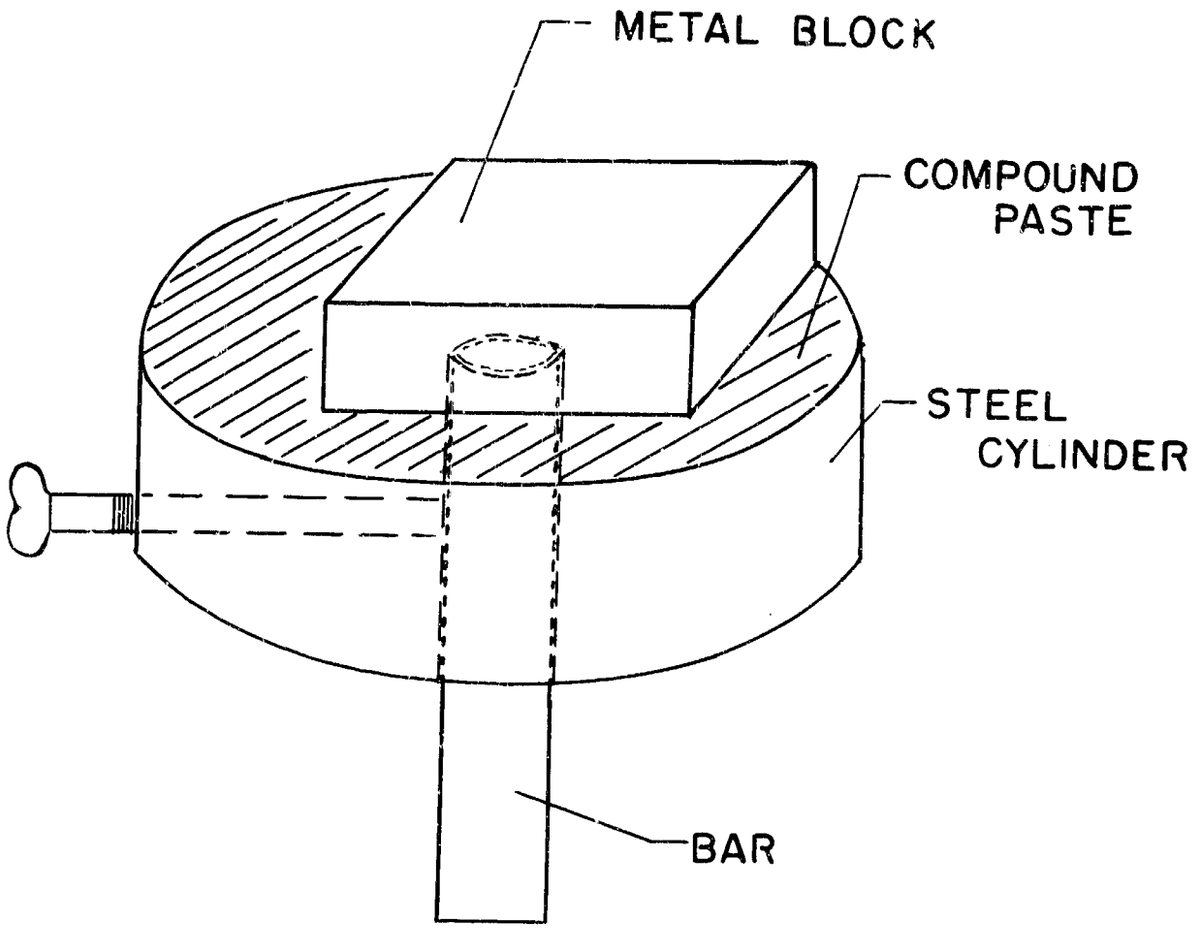

FIG. 4 LAPPING TOOL

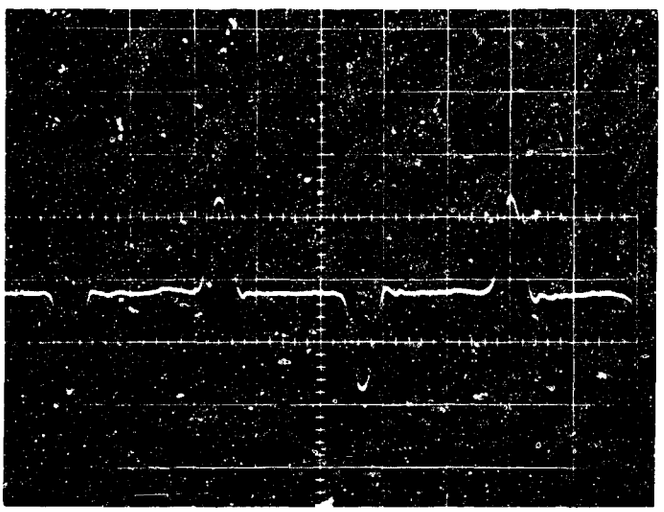

50 $\frac{\mu sec}{cm}$

1 $\frac{mV}{cm}$

Fig. 5 - Pulse propagation and reflection in a single steel bar.

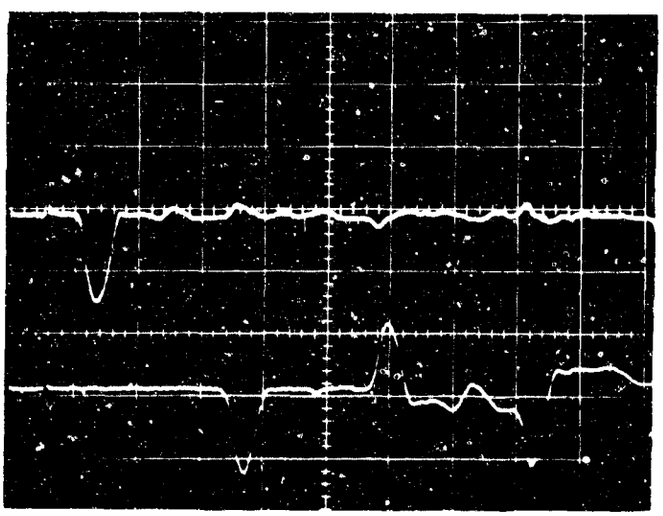

50 $\frac{\mu sec}{cm}$

1 $\frac{mV}{cm}$

Fig. 6 - Pulse propagation in two steel bars attached end to end.

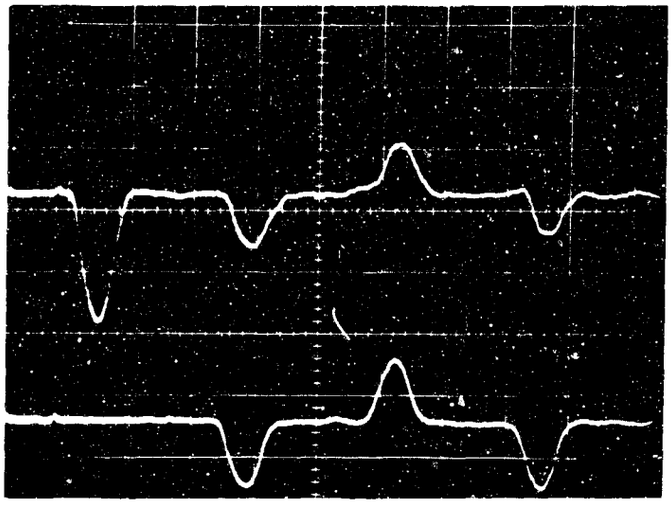

Fig. 7 - Propagation of stress pulse from aluminum to steel.

Fig. 8 - Propagation of stress pulse from steel to aluminum.

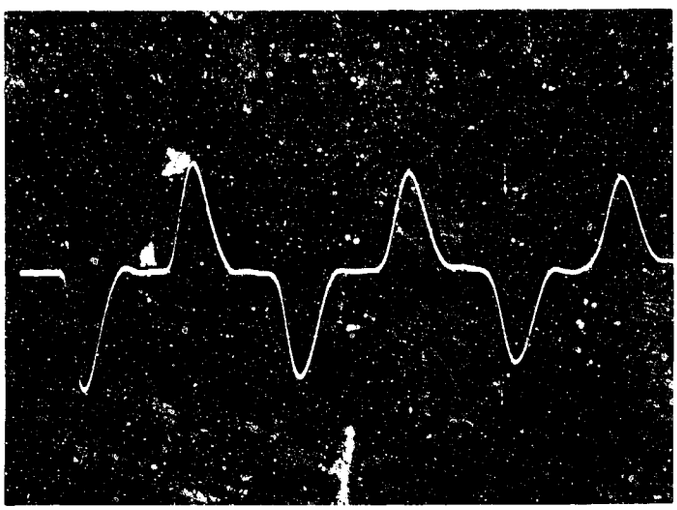

Fig. 9 - Pulse propagation and reflection in single polystyrene bar.

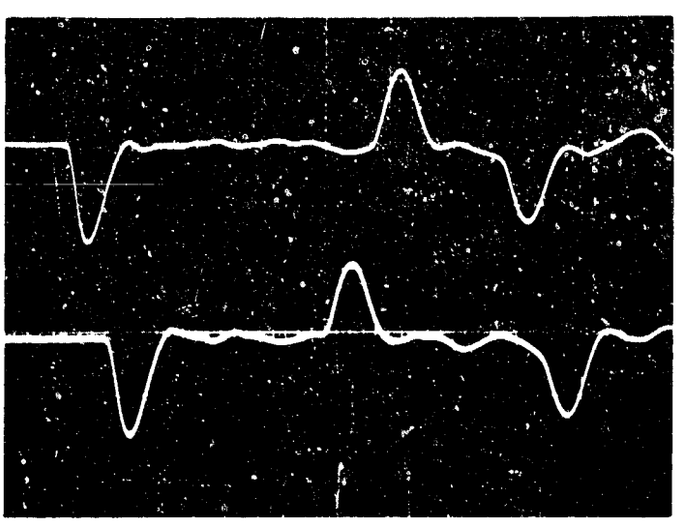

Fig. 10 - Pulse propagation in two polystyrene bars attached end to end.

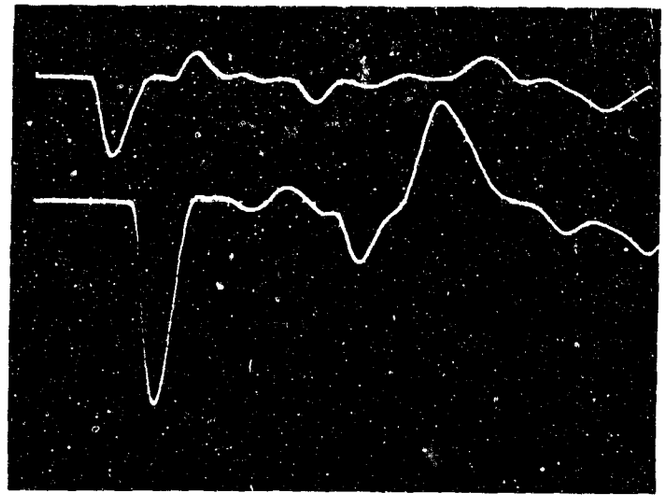

200 $\frac{\mu sec}{cm}$

2 $\frac{mV}{cm}$

Fig. 11 - Propagation of stress pulse from polystyrene to polyethylene.

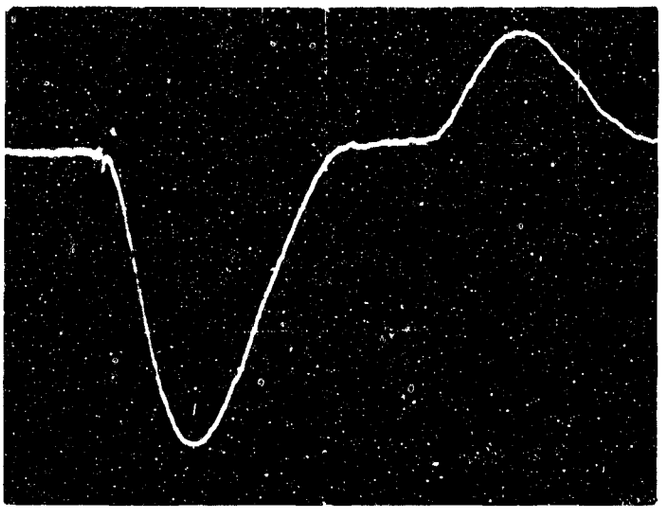

Fig. 12a - Incident and reflected pulses in polystyrene bar attached to polyethylene bar (1st experiment).

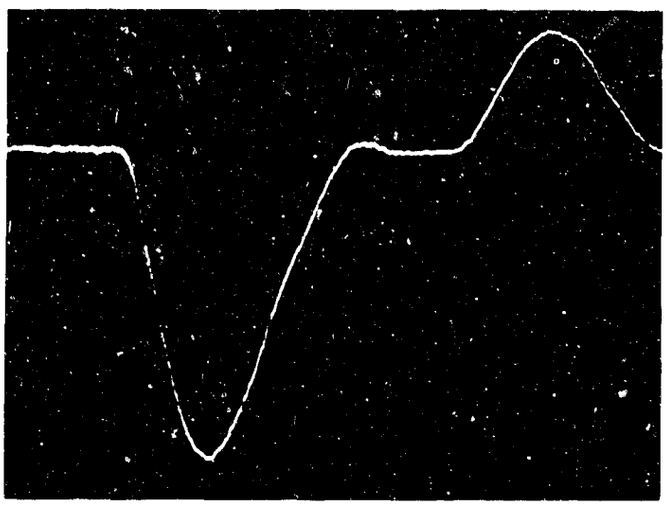

Fig. 12b - Incident and reflected pulses in polystyrene bar attached to polyethylene bar (2nd experiment).

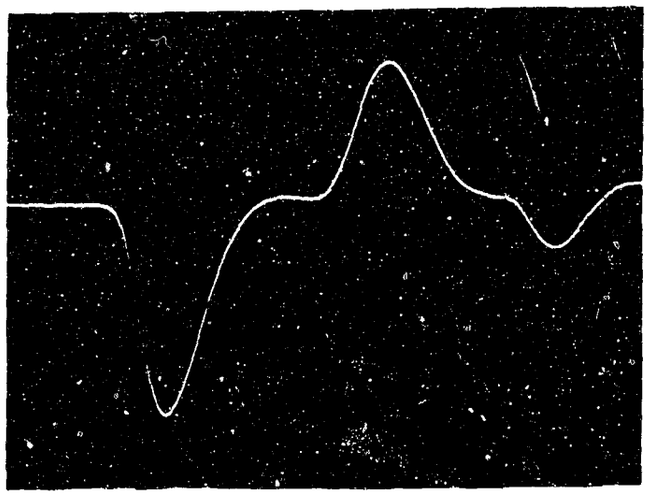

100 $\frac{\mu sec}{cm}$

2 $\frac{mV}{cm}$

Fig. 13 - Transmitted pulse in polyethylene bar

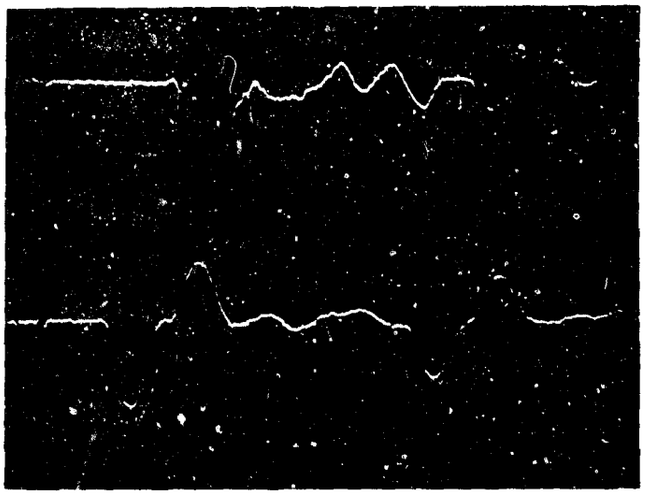

50 $\frac{\mu sec}{cm}$

0.5 $\frac{mV}{cm}$

Fig. 14 - Propagation of stress pulse from aluminum to Lucite (p.m.m.)

10 $\frac{\mu sec}{cm}$

0.2 $\frac{mV}{cm}$

Fig. 15 - Incident and reflected pulses in aluminum bar attached to Lucite bar

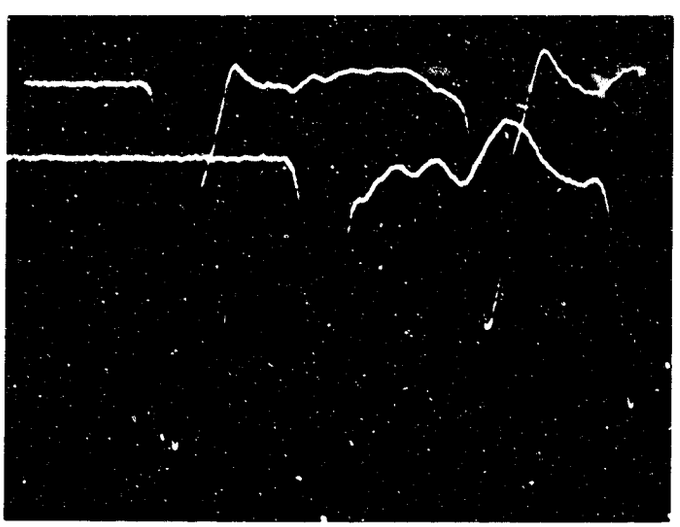

50 $\frac{\mu sec}{cm}$

0.5 $\frac{mV}{cm}$

Fig. 16 - Recording of transmitted pulse in Lucite bar by two strain gages mounted $9\frac{1}{2}$" apart.

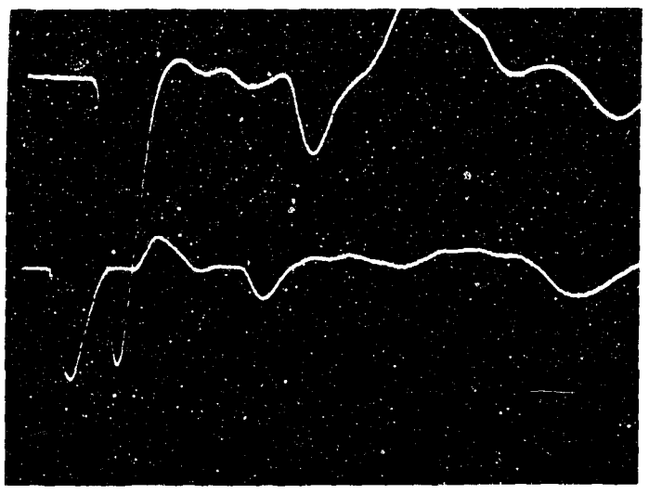

200 $\frac{\mu sec}{cm}$

1 $\frac{mV}{cm}$

Fig. 17 - Propagation of stress pulse from polystyrene to green solid propellant (g.s.p.)

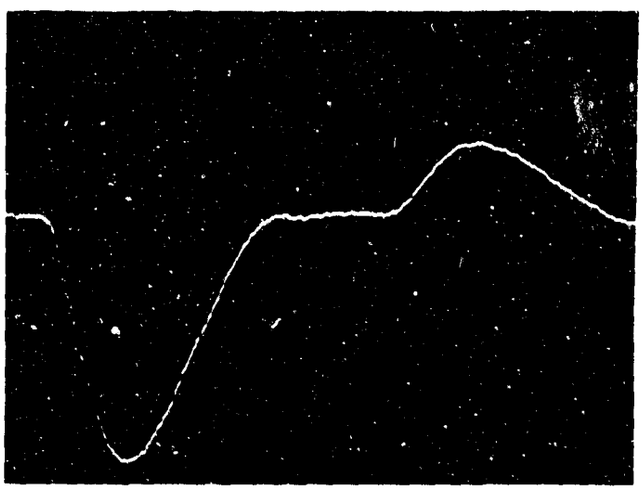

50 $\frac{\mu sec}{cm}$

0.5 $\frac{mV}{cm}$

Fig. 18 - Incident and reflected pulses in polystyrene bar attached to g.s.p. bar

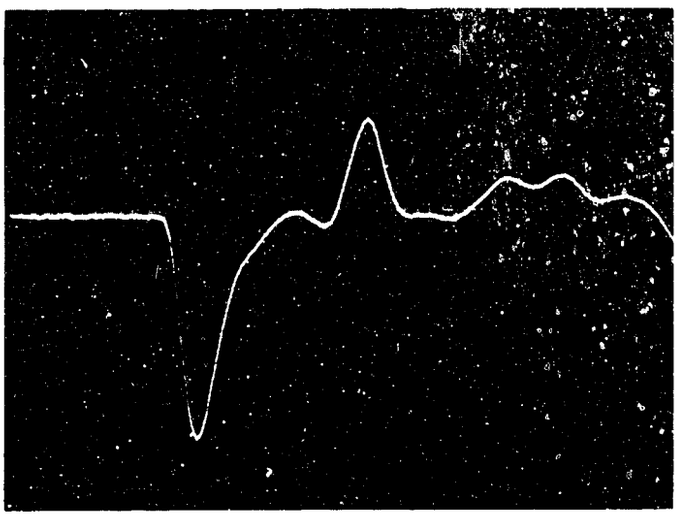

200 $\frac{\mu sec}{cm}$

1 $\frac{mV}{cm}$

Fig. 19 - Transmitted pulse in g.s.p. bar

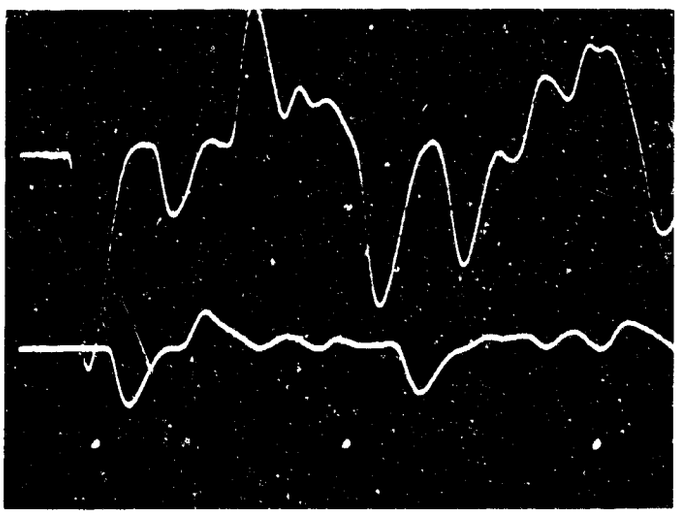

200 $\frac{\mu sec}{cm}$

1 $\frac{mV}{cm}$

Fig. 20 - Propagation of stress pulse from polystyrene to pine wood

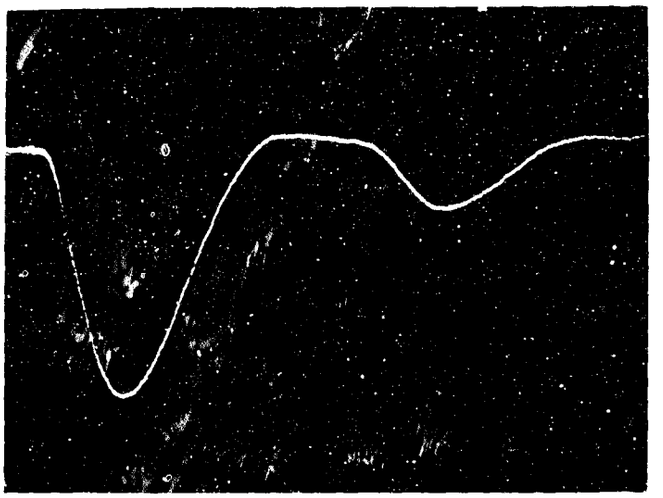

50 $\frac{\mu sec}{cm}$

1 $\frac{mV}{cm}$

Fig. 21 - Incident and reflected pulses in polystyrene bar attached to pine wood bar

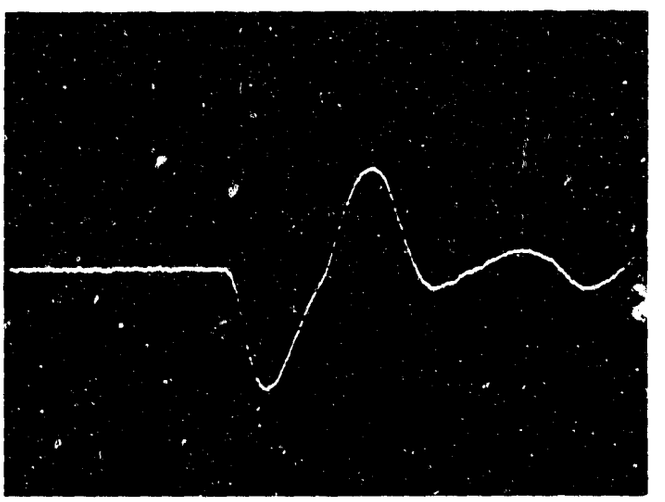

100 $\frac{\mu sec}{cm}$

0.5 $\frac{mV}{cm}$

Fig. 22 - Transmitted pulse in pine wood bar

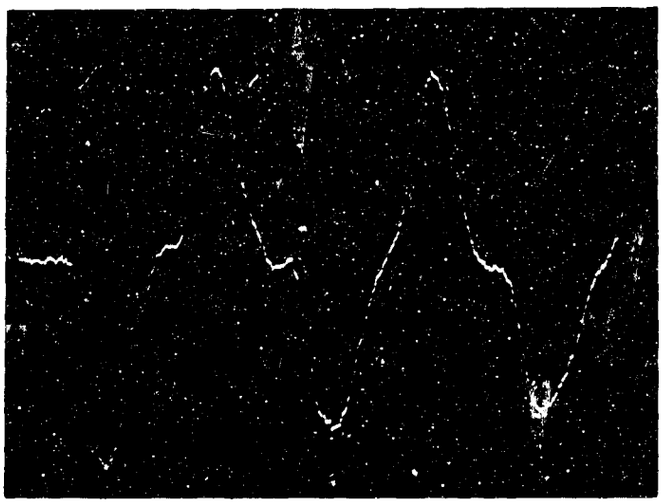

100 $\frac{\mu sec}{cm}$

0.2 $\frac{mV}{cm}$

Fig. 23 - Propagation of stress pulse in a single pine wood bar

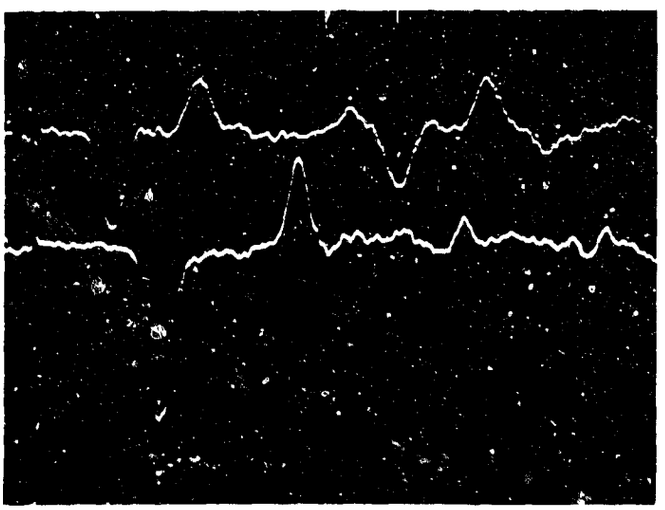

50 $\frac{\mu sec}{cm}$

0.2 $\frac{mV}{cm}$

Fig. 24 - Propagation of stress pulse from steel to sandstone

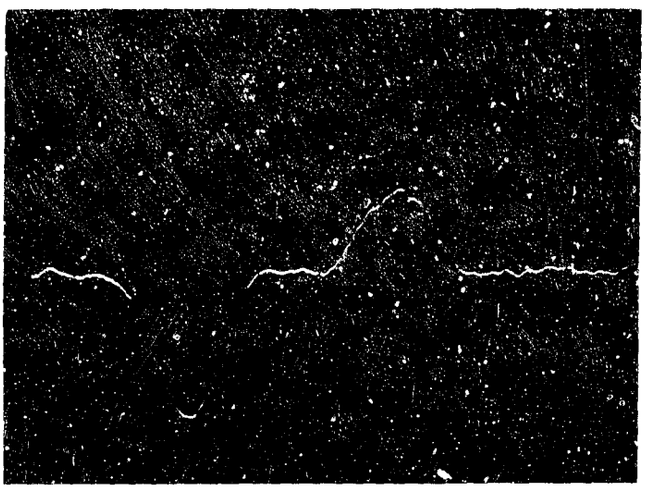

Fig. 25 - Incident and reflected pulses in steel bar attached to sandstone bar

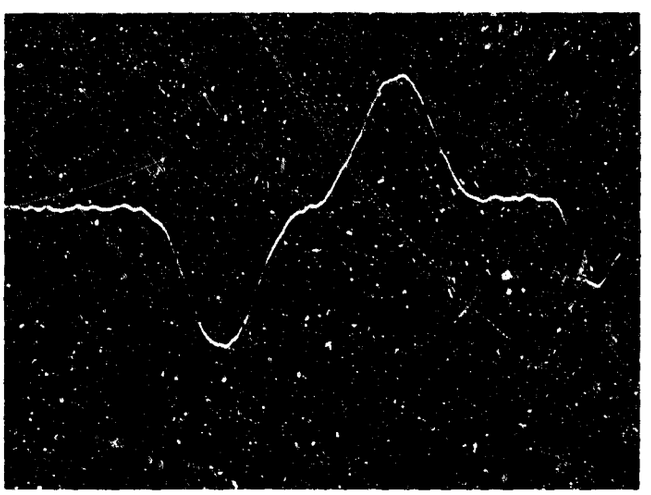

Fig. 26 - Transmitted pulse in sandstone bar

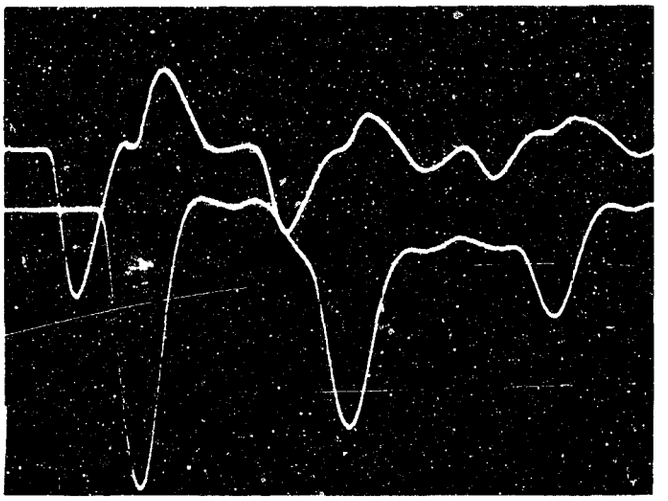

200 $\frac{\mu sec}{cm}$

1 $\frac{mV}{cm}$

Fig. 27 - Propagation of stress pulse from polystyrene to clay

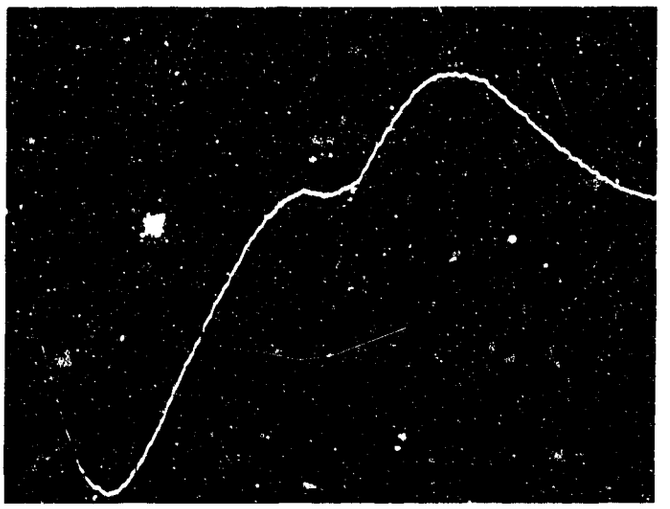

50 $\frac{\mu sec}{cm}$

0.5 $\frac{mV}{cm}$

Fig. 28 - Incident and reflected pulses in polystyrene bar attached to clay bar

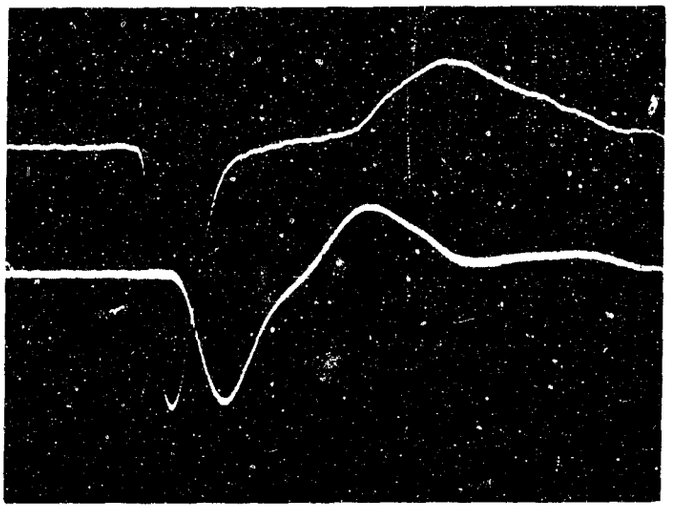

200 $\frac{\mu sec}{cm}$

1 $\frac{mV}{cm}$

Fig. 29 - Recording of transmitted pulse in clay by two strain gages mounted 8 cm apart

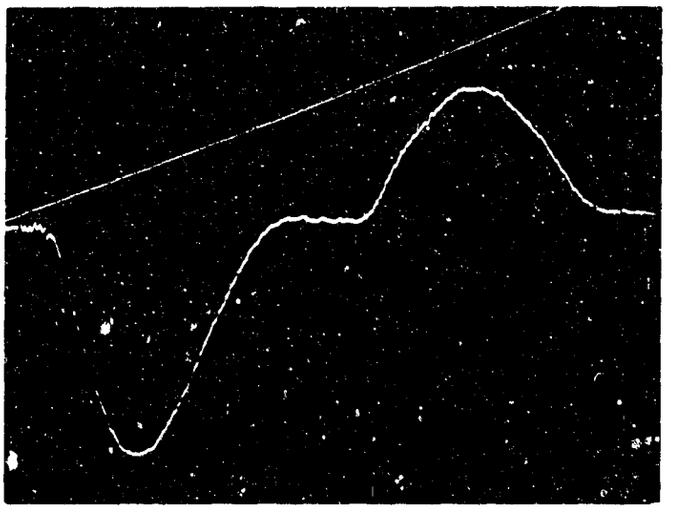

50 $\frac{\mu sec}{cm}$

0.5 $\frac{mV}{cm}$

Fig. 30 - Incident and reflected pulses in polystyrene bar attached to wet sand bar

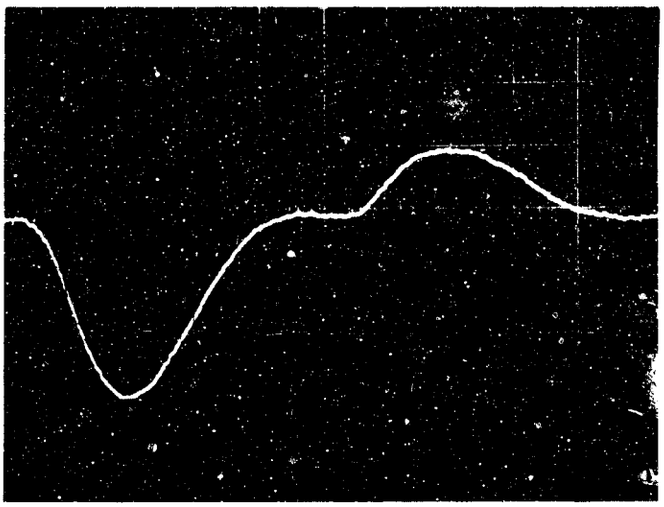

50 $\frac{\mu sec}{cm}$

0.5 $\frac{mV}{cm}$

Fig. 31 - Incident and reflected pulses in polystyrene bar attached to dry sand bar

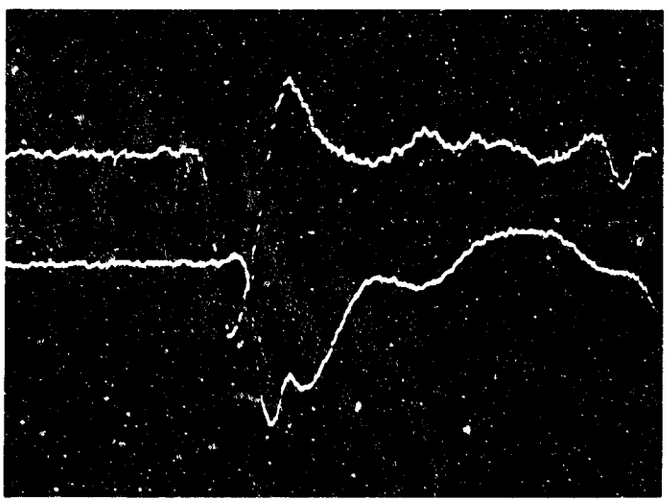

100 $\frac{\mu sec}{cm}$

0.2 $\frac{mV}{cm}$

Fig. 32 - Recording of transmitted pulse in dry sand bar by two strain gages mounted 3.5 cm apart

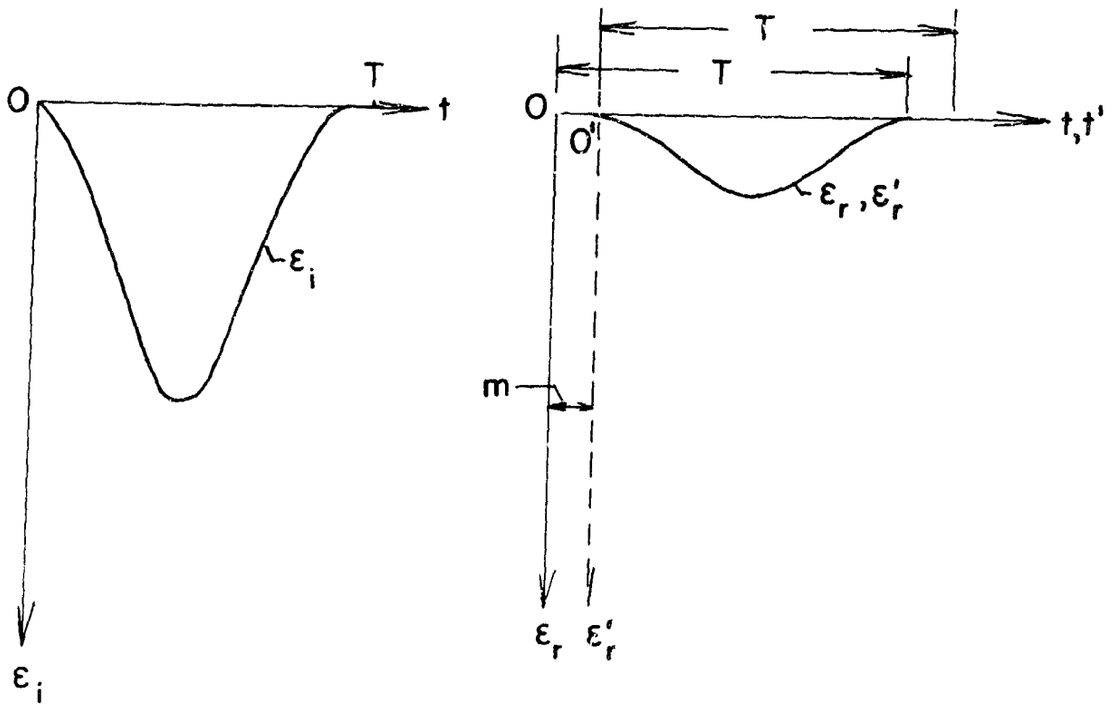

INCIDENT PULSE REFLECTED PULSE

FIG. 33. POSTULATED STRAIN PULSES FOR SHOWING EFFECT OF SHIFT

$$\varepsilon_i(t) = 0.0687\, e^{0.019(2.4-t)}\, t^{1.2}(2\pi - t)^{1.2}$$

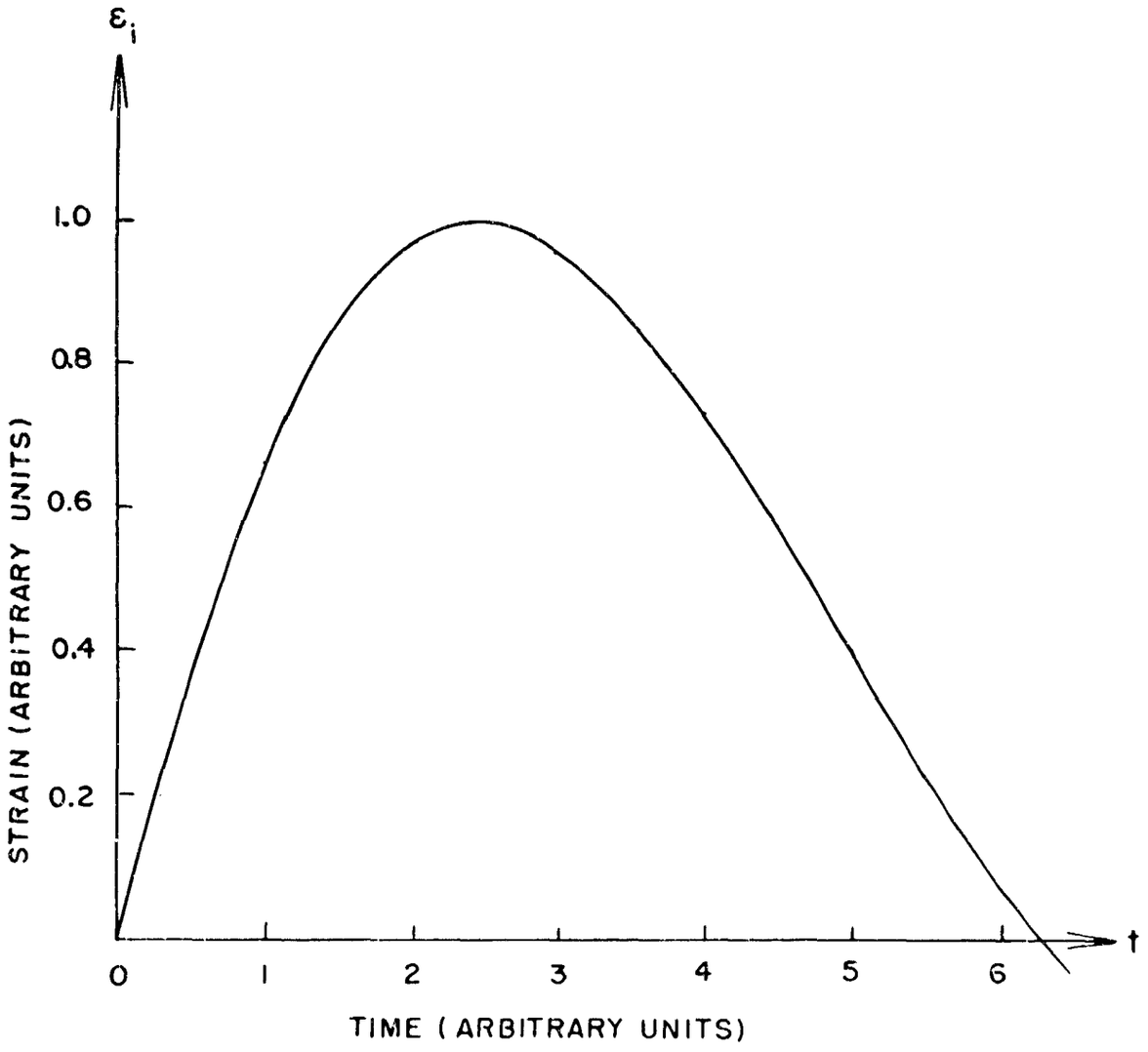

FIG. 34 INCIDENT PULSE

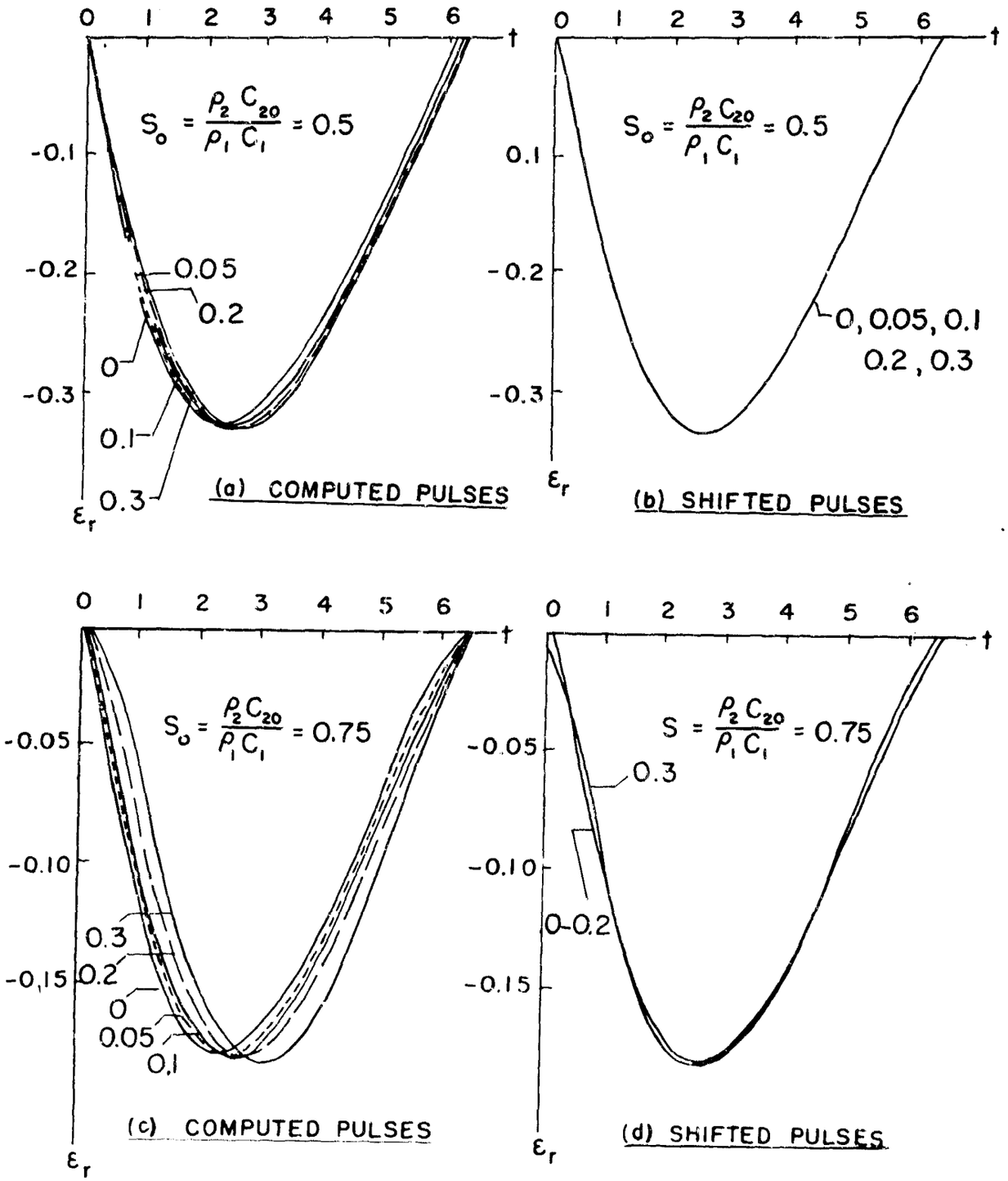

FIG. 35 REFLECTED PULSES FOR DIFFERENT VALUES OF TAN δ'

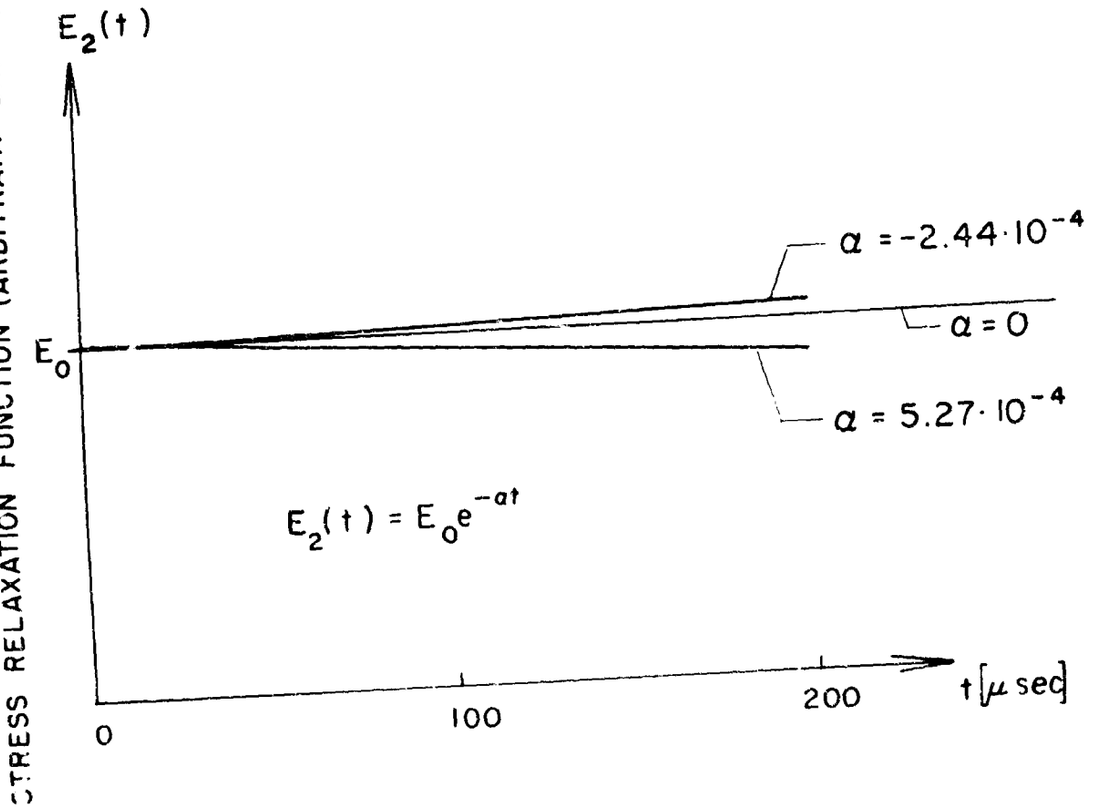

FIG. 36 STRESS RELAXATION FUNCTION

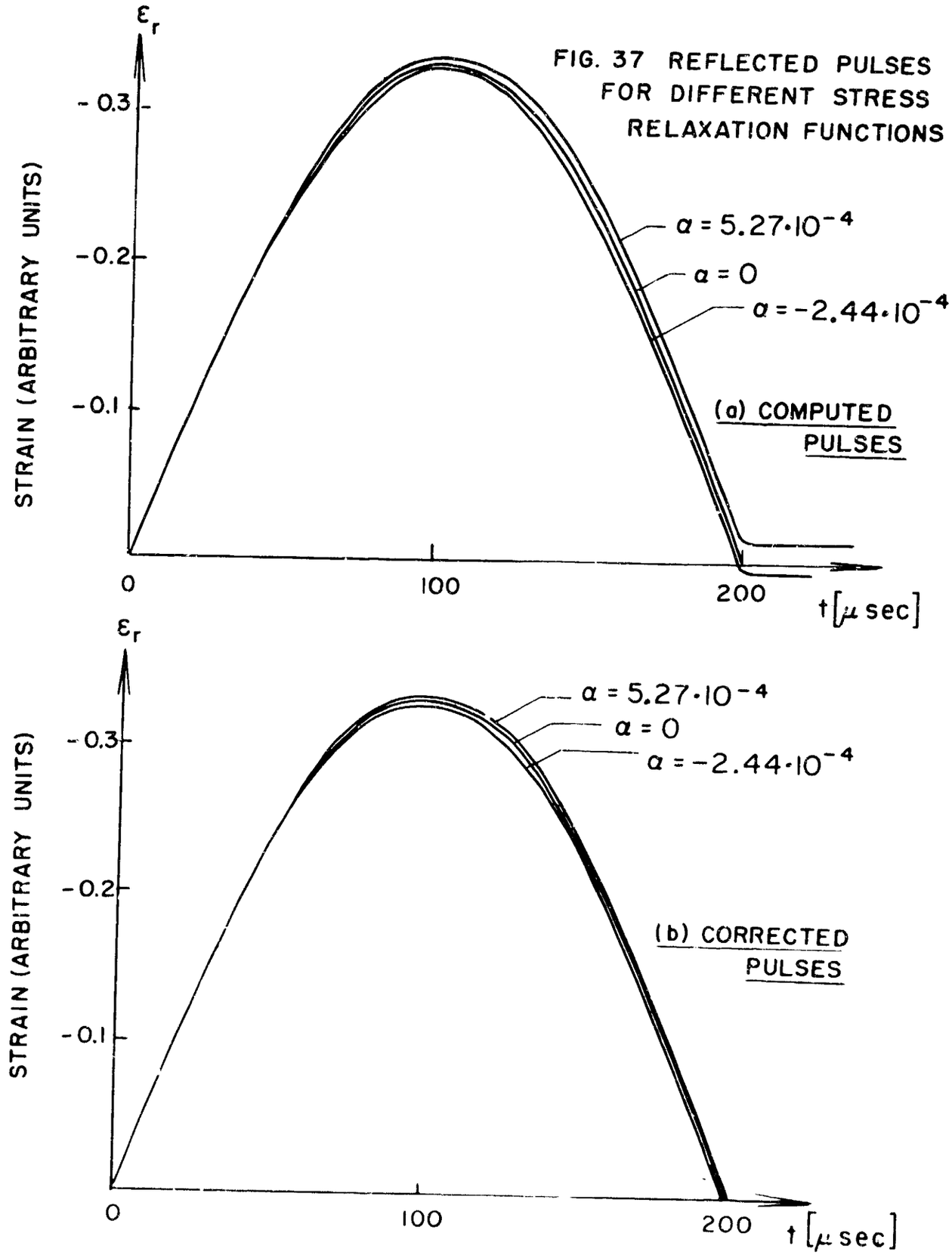

FIG. 37 REFLECTED PULSES FOR DIFFERENT STRESS RELAXATION FUNCTIONS

Unclassified
Security Classification

DOCUMENT CONTROL DATA - R & D

(Security classification of title, body of abstract and indexing annotation must be entered when the overall report is classified)

1. ORIGINATING ACTIVITY *(Corporate author)*
Brown University

2a. REPORT SECURITY CLASSIFICATION
Unclassified

2b. GROUP
NA

3. REPORT TITLE
Experimental Technique for Determining Some Dynamic Properties of Viscoelastic Materials.

4. DESCRIPTIVE NOTES *(Type of report and inclusive dates)*
Technical Report

5. AUTHOR(S) *(First name, middle initial, last name)*
Amnon Meer

6. REPORT DATE
Feb 69

7a. TOTAL NO. OF PAGES
119

7b. NO. OF REFS
11

8a. CONTRACT OR GRANT NO.
DA-31-124-ARO-D-358

b. PROJECT NO.
2006 1102-B336

c.

d.

9a. ORIGINATOR'S REPORT NUMBER(S)

9b. OTHER REPORT NO(S) *(Any other numbers that may be assigned this report)*
5606.9-E

10. DISTRIBUTION STATEMENT
This document has been approved for public release and sale; its distribution is unlimited.

11. SUPPLEMENTARY NOTES
None

12. SPONSORING MILITARY ACTIVITY
U.S. Army Research Office-Durham
Box CM, Duke Station
Durham, North Carolina 27706

13. ABSTRACT

~~In this report~~, an experimental technique is described, by which some basic properties of viscoelastic materials such as phase velocity, loss factor and stress relaxation function could be derived. The technique is based on the propagation and reflection of longitudinal stress pulses in a system of two bars one of which is elastic with known properties and the other viscoelastic with properties to be determined. It is shown that the unknown properties of the viscoelastic bar may be determined from the shapes of the incident and reflected stress pulses which travel in the elastic bar. It turns out however that the only material property which may be derived with reasonable accuracy is the phase velocity for the basic frequency of the pulses propagating along the bars. All the other material properties proved to be extremely sensitive to small experimental errors and hence no reliable values for them could be derived.

KEY WORDS:

Viscoelasticity
Viscoelasticity-Mechanical Properties
Materials Tests-Tests
Materials Tests-Mechanical Tests

DD FORM 1 NOV 68 1473 REPLACES DD FORM 1473, 1 JAN 64, WHICH IS OBSOLETE FOR ARMY USE.

Unclassified
Security Classification